Published in final edited form as:

Nature. 2019 July ; 571(7764): 205–210. doi:10.1038/s41586-019-1362-5.

Single cell analysis reveals T cell infiltration in old neurogenic niches

Ben W. Dulken[1,2,3,*], **Matthew T. Buckley**[1,*], **Paloma Navarro Negredo**[1,*], **Naresha Saligrama**[4,5], **Romain Cayrol**[6], **Dena S. Leeman**[1,7], **Benson M. George**[2,3], **Stéphane C. Boutet**[8], **Katja Hebestreit**[1], **John V. Pluvinage**[9], **Tony Wyss-Coray**[9], **Irving L. Weissman**[3], **Hannes Vogel**[6], **Mark M. Davis**[4,5,10], **Anne Brunet**[1,11,12]

[1]Department of Genetics, Stanford University, Stanford CA 94305

[2]Stanford Medical Scientist Training Program, Stanford University, Stanford CA 94305

[3]Institute for Stem Cell Biology and Regenerative Medicine, Stanford University, Stanford CA 94305

[4]Department of Immunology and Microbiology, Stanford CA 94305

[5]Institute for Immunity, Transplantation and Infection, Stanford University School of Medicine, Stanford CA 94305

[6]Department of Pathology, Stanford University School of Medicine, Stanford CA 94305

[7]Cancer Biology Program, Stanford University, Stanford CA 94305

[8]Fluidigm Corporation, South San Francisco, CA 94080

[9]Department of Neurology and Neurological Sciences, Stanford University School of Medicine, Stanford, CA 94305

[10]Howard Hughes Medical Institute

[11]Glenn Laboratories for the Biology of Aging at Stanford University

Abstract

The mammalian brain contains neurogenic niches comprising neural stem cells (NSCs) and other cell types. Neurogenic niches become less functional with age, but how they change during aging remains unclear. Here we perform single cell RNA-sequencing of young and old neurogenic

[12]Corresponding author: abrunet1@stanford.edu.

Author Contributions

B.W.D. and A.B. planned the study. B.W.D. performed and analyzed most experiments, except those indicated below. M.T.B. performed one 10x Genomics and Smart-seq v4 replicate and analyzed the combined data. P.N.N. designed and analyzed human brain experiments and performed and analyzed immunocytochemistry *in vivo* and in culture. N.S. performed TCR sequencing by nested PCR and MOG injection under the supervision of M.M.D.. R.C. and H.V. provided human brain tissues and helped with design. S.C.B. helped with Fluidigm C1 libraries. D.S.L. helped with the NSC FACS protocol. K.H. helped with statistical analysis. B.M.G., J.V.P, T.W.-C., I.L.W., and M.M.D. provided intellectual contribution. B.W.D. and A.B. wrote the initial manuscript, and M.T.B. and P.N.N. wrote the revised version.

*These authors contributed equally to this work

Competing interests. The authors declare no competing interests.

niches in mice. Analysis of 14,685 single cell transcriptomes reveals a decrease in activated NSCs, changes in endothelial cells and microglia, and infiltration of T cells in old neurogenic niches. Surprisingly, T cells in old brains are clonally expanded and generally distinct from those in old blood, suggesting they may experience specific antigens. T cells from old brains express interferon γ, and the subset of NSCs with a high interferon response shows decreased proliferation *in vivo*. Interestingly, T cells can inhibit NSC proliferation in co-cultures and *in vivo*, in part by secreting interferon. Our study reveals an interaction between T cells and NSCs in old brains, opening potential avenues to counter age-related decline in brain function.

Main

A hallmark of aging is a decline in tissue function, but how changes in cell composition affect tissue function is largely unknown. The adult subventricular zone (SVZ) neurogenic niche provides a great paradigm to address this question, as it contains different cell types (astrocytes, NSCs at different stages of commitment, endothelial cells, microglia) and exhibits functional decline during aging[1-16]. Age-dependent changes in this neurogenic niche have previously been documented[7-16]. However, a systematic examination at single cell resolution of the changes that occur in this neurogenic region with aging has never been done.

Single cell RNA-seq analysis of young and old neurogenic niches

Single cell RNA-sequencing analyses have been performed on young[17-24] and old neural stem cell lineages[25,26], but a single cell understanding of the aging neurogenic niche is missing. To address this gap, we performed single cell RNA-sequencing (RNA-seq) of the entire SVZ in three young (3 months) and three old (28–29 months) mice in three independent experiments (Fig. 1a, b). Young and old animals were perfused to remove the blood, and cells were rapidly dissociated from SVZ niches and FACS-sorted to eliminate debris (Fig. 1a, b). Single cell RNA-seq was performed on the entire SVZ niche using the 10x Genomics Chromium platform (Fig. 1a, b, Extended Data Fig. 1a, Supplementary Tables 1, 2). Analysis of 14,685 high quality single cell transcriptomes with tSNE projection revealed 11 distinct cell types in the neurogenic niche (Fig. 1a). Characterization of markers in these clusters (Extended Data Fig. 1b) identified them as astrocytes/quiescent neural stem cells (qNSCs), activated neural stem cells (aNSCs)/neural progenitors (NPCs), neuroblasts (NBs), neurons, oligodendrocyte progenitor cells (OPCs), oligodendrocytes, endothelial cells, ‘mural’ cells (e.g. pericytes), microglia, macrophages, and T cells (Fig. 1a, b). Interestingly, the T cell population was almost exclusively from old mice (Fig. 1b, Extended Data Fig. 1c), and T cells were strikingly enriched in old SVZ (Fig. 1c, Supplementary Table 3). Old age was also accompanied with a decreased number of aNSCs/NPCs and neuroblasts (Fig. 1b, c, Supplementary Table 3), as previously shown[7-15] (though quantification of single cell data could be influenced by differential dissociation properties with age), and shifts in the transcriptomic states of microglia, endothelial cells, and oligodendrocytes[26] (Fig. 1b, d, Supplementary Table 3).

Immunofluorescence staining confirmed that T cells were increased in old neurogenic regions, in close proximity to NSCs (Fig. 1e, f). These T cells did not co-localize with

endothelial cells (Extended Data Fig. 2a), indicating that T cells were not in blood vessels, but within the brain parenchyma. T cell invasion in old brain coincided with the age-dependent decline in aNSCs in the neurogenic niche (Fig. 1e, g). Hence, T cells and NSCs could influence each other in old brains.

Single cell data analysis revealed that T cells in old brains expressed markers of CD8 positive T cells (*Cd8+Cd4-*) (Fig. 1h, i), and FACS analysis confirmed that old neurogenic niches were infiltrated by CD3+CD8+CD4- T cells (Fig. 1j, k). T cells in old brains also expressed markers of effector memory cells (*Cd62L*^{low}, *Cd44*^{high}), tissue retention (*Itgal, Itga4*), and activation (*Cd69, Xcl1*), including cytokines such as interferon γ (*Ifng*) (Fig. 1i)[27]. In fact, T cells were the only prominent source of interferon transcripts detected in this single cell analysis (Fig. 1h, Extended Data Fig 2b).

Interestingly, brains from old humans, even in the absence of neurodegenerative diseases, also exhibited infiltration of CD8+ T cells in the region lining the lateral ventricle – a region with neurogenic potential[16] (Fig. 1l, m, Extended Data Fig. 2c, Supplementary Table 4). Thus, infiltration of T cells in old brains also occurs in humans.

T cells invading old brains are clonally expanded

To characterize the T cells in old brains, we purified CD8+ T cells from the neurogenic niche and blood of the same mouse in four different old mice and performed whole transcript single cell RNA-sequencing using Smart-seq v4. T cells in the old neurogenic niche differed from those in the blood of the same old individual (Fig. 2a, Extended Data Fig. 3a, b, Supplementary Tables 5, 6). Unlike their counterpart from old blood, T cells from old niches expressed high levels of IFNγ and the immune checkpoint PD1 (Fig. 2b, Extended Data Fig. 3c, Supplementary Tables 5, 6).

A key question is whether T cells infiltrate the old brain passively due to the age-related disruption of the blood-brain-barrier[28], or whether they actively recognize antigens in old brains. When T cells recognize an antigen, they clonally expand, with each clone expressing the same T cell receptor (TCR)[29]. To test T cell clonality, we extracted TCR sequences from single T cell transcriptomes (Fig. 2a, c). Surprisingly, TCR analysis from 4 different old mice revealed that several T cells in old neurogenic niches were clonally expanded (Fig. 2c, e, f, Extended Data Fig. 3d, Supplementary Table 7). The TCR repertoire of old brain T cell clones was different from that of old blood (Fig. 2c, f), suggesting that they did not simply originate from passive diffusion through a disrupted blood-brain-barrier with aging. We confirmed that T cells from old brains were clonally expanded and differed from that of old blood using nested PCR (Fig. 2d, Extended Data Fig. 3e, g, h; Supplementary Table 7). Thus, T cells in old brains are clonally expanded and differ from those in old blood in that they express different TCRs and exhibit high levels of IFNγ transcripts.

The neurogenic niche responds to IFN signaling

Interferons are important for the defense against pathogens[30] and abnormal endogenous nucleotides[31,32]. The effect of interferons has been examined in the developing brain and adult neurogenic niche[26,33-36], but the role of IFNγ has remained unclear. Analysis of our single cell data reveal that several cell types in the neurogenic niche (astrocytes/qNSCs,

aNSCs/NPCs, endothelial cells, and microglia) expressed the IFNγ receptor (Extended Data Fig. 4a, b) and exhibited an age-associated increase in the IFNγ response signature (e.g. *Ifit1*, *Stat1*, and *Bst2*, Supplementary Table 8) (Fig. 3a, b, Extended Data Fig. 4c, d, h-j). Immunofluorescence staining and FACS revealed strongly elevated staining for STAT1 – a protein that is upregulated upon interferon signaling[33]– in old aNSCs/NPCs, microglia, and endothelial cells (Fig. 3c-e, Extended Data Fig. 4e, f). Hence, multiple cell types in the old neurogenic niche, including NSCs, experience a strong response to IFNγ – though they may also be responding to other interferons[26].

IFNγ signaling from T cells negatively impacts NSCs

We characterized NSC response to IFNγ. Principal component analysis (PCA) using only genes associated with the IFNγ response revealed that a subpopulation of old astrocytes/qNSCs and aNSCs/NPCs experience a high IFNγ response (Extended Data Fig. 5a-c, Supplementary Table 9). FACS analysis validated that only a subpopulation of old qNSCs and aNSC/NPCs exhibited elevated STAT1 staining (Extended Data Fig. 5d). Thus, old NSCs exhibit a heterogeneous IFNγ response.

We next determined if the subpopulation of old NSCs exhibiting a strong IFNγ response differs from its non-responsive counterpart. To isolate this subpopulation, we searched for a surface marker that correlated with the IFNγ response and identified *Bst2/Tetherin*, which encodes a surface protein involved in viral vesicle budding in response to interferons[37-39] (Extended Data Fig. 5e). FACS analysis confirmed that a subpopulation of aNSCs/NPCs from old mice showed increased BST2 expression (Fig. 4a, Extended Data Fig. 5f, g). Bulk RNA-seq analysis validated that the BST2-positive subpopulation of old aNSCs/NPCs was strongly enriched for genes associated with the IFNγ response compared to its BST2-negative counterpart (Fig. 4b, Supplementary Tables 10, 11). The subpopulation of BST2-positive aNSCs/NPCs from old mice was depleted in transcripts related to the cell cycle compared to its counterpart (Fig. 4b). To assess the proliferation status of the subset of old NSCs experiencing a high IFNγ response, we injected old mice with EdU (5-ethynyl-2'-deoxyuridine), which incorporates in proliferating cells. The BST2-positive subpopulation of old aNSCs/NPCs exhibited reduced EdU incorporation and decreased staining for KI67 (another marker of cycling cells) compared to its BST2-negative counterpart (Fig. 4c, Extended Data Fig. 5h). Thus, the subset of old NSCs that experiences a strong IFNγ response is dysfunctional *in vivo*.

We asked if T cells could contribute to the high interferon response in NSCs and impact their proliferation. The presence of T cells in the neurogenic niche was correlated with an increase in BST2 in the NSCs that are in proximity to these T cells (Fig. 4d, e). Forcing CD8+ T cell entry into the brain of young mice by injecting a brain-specific antigen (myelin oligodendrocyte glycoprotein, MOG)[40,41] (Extended Data Fig. 6a-c) was associated with an increase in BST2 expression in aNSCs/NPCs and a concomitant reduction in proliferation *in vivo* (Extended Data Fig. 6d, e). While MOG also induces other immune responses[40,41], these results suggest that T cells impair NSC proliferation *in vivo*.

To test whether T cells can directly impact NSC proliferation, we co-cultured CD8+ T cells with NSCs isolated from young mice (Fig. 4f). Immunofluorescence and FACS analyses

both indicated that the addition of T cells, in the presence of a cytokine cocktail that promotes IFNγ production in T cells[42], induced BST2/Tetherin expression in NSCs (Fig. 4g, h) and strikingly reduced NSC proliferation (Fig. 4g, i). Both the induction of BST2/Tetherin and the reduction in NSC proliferation in the presence of activated T cells were reversed by a neutralizing antibody to IFNγ (Fig. 4g-i). Similar effects were observed when T cells were activated using antibodies to CD3 and CD28 (Extended Data Fig. 6f, g). Thus, T cells can directly inhibit NSC proliferation via secretion of IFNγ, although other cells, such as microglia or endothelial cells, could also contribute to NSC dysfunction *in vivo*.

Discussion

Our study provides a systems-level understanding of the old neurogenic niche in the mammalian brain and shows that T cells infiltrate this niche with age. Intriguingly, these T cells are clonally expanded and differ from blood T cells, suggesting that they may recognize a specific antigen in the old brain. T cells were recently shown to infiltrate the brain in the context of neurodegenerative diseases[43-45] and during aging[46,47]. However, their clonal expansion in the old neurogenic niche had never been reported. T cells infiltrated in old neurogenic niches might recognize neo-antigens, including those from aggregated proteins in old NSCs[14]. Other cells in the old neurogenic niche, such as microglia[48], endothelial cells[49], or other immune cells in the brain such as macrophages[47] could provide chemokines to attract T cells.

While T cells can influence the nervous system during development and youth[36,50-52], and during disease (e.g. infection[53,54] or multiple sclerosis[40,41]), their role during aging is not clear. We show that brain T cells express IFNγ and that several cells in the niche, including NSCs, exhibit an IFNγ response. The IFNγ response induced by T cells appears to be detrimental for NSC function *in vitro* and *in vivo*. Although the exact link between T cells, interferon, and NSC proliferation remains to be established, our results provide a possible cause for the decline of NSC during aging and suggest avenues to counter age-associated cognitive impairment.

Methods

Laboratory animals

All mice used in this study were male C57BL/6 mice. For experiments using paired young and old mice, or old mice alone, mice were obtained from the NIA Aged Rodent colony. For experiments done exclusively in young mice, mice were obtained from the Jackson Laboratory. Mice were habituated for >1 week at Stanford before use. At Stanford, all mice were housed in the Comparative Medicine Pavilion or the Research Animal Facility II, and their care was monitored by the Veterinary Service Center at Stanford University under IUCAC protocols #8661 and #28396.

Single cell RNA-seq from young and old SVZ using 10x Genomics Chromium

We performed single cell RNA-sequencing of all live cells in the subventricular zone (SVZ) neurogenic niche. To this end, we used three young (3 months), and three old (28–29 months) male C57BL/6 mice from the NIA aged colony in three independent experiments,

performed by two independent investigators (B.W.D. performed the first two experiments, and M.T.B. performed the third experiment). Specifically, mice were sedated and perfused with 20 ml of PBS with heparin sodium salt (50 U/mL) (Sigma Aldrich) to remove the blood, and brains were immediately harvested. As described in [4], the SVZ from each hemisphere was micro-dissected and dissociated with enzymatic digestion with papain for 10 min at a concentration of 14U/mL. The dissociated SVZ was then triturated in a solution containing 0.7mg/mL ovomucoid, and 0.5mg/mL DNAseI in DMEM/F12. The dissociated cells from the SVZ were then centrifuged through 22% Percoll in PBS to remove myelin debris. Following centrifugation through Percoll solution, cells were washed with FACS buffer (HBSS, 1% BSA, 0.1% Glucose). Live/dead staining was performed using 1μg/mL propidium iodide (Biolegend). FACS sorting was performed on a BD FACS Aria II sorter, using a 100μm nozzle at 13.1 PSI. Cells were sorted into catching media: DMEM/F12 (ThermoFisher) with B27 supplement (ThermoFisher, no Vitamin A, 1:50), N2 supplement (ThermoFisher, 1:100), 15mM HEPES buffer, 0.6% glucose, Penicillin-Streptomycin-Glutamine (Life Technologies, 1:100), and Insulin-Transferrin-Selenium (Life Technologies, 1:1000). Cells were then spun down at 300xg for 5 minutes at 4°C and resuspended in catching media at a concentration of 300 cells/μL.

Cells were loaded onto a 10x Genomics Chromium chip per factory recommendations. Reverse transcription and library preparation was performed using the 10x Genomics Single Cell v2 kit following the 10x Genomics protocol. One young and one old library were multiplexed and sequenced on one lane of Illumina NextSeq-500 with a high output (400m) kit.

Quality control of 10x Genomics single cell RNA-seq

For mapping, sequences obtained from sequencing using the 10x Genomics single cell RNA-sequencing platform were demultiplexed and mapped to the mm10 transcriptome using the Cell Ranger package (10x Genomics). Cells were removed if they were expressing fewer than 400 unique genes, more than 4,500 unique genes, or greater than 15% mitochondrial reads. Genes not detected in any cell were removed from subsequent analysis. Levels of mitochondrial reads and numbers of Unique molecular identifiers (UMIs) were similar between the young and old conditions (Supplementary Table 2), indicating that there were no systematic biases in the libraries from young and old mice. Average gene detection in each cell type was similar between young and old (Extended Data Fig. 1a). Our study includes 14,685 cells, with 8,884 cells from young (Young 1: 2,306, Young 2: 2,675, Young 3: 3,903) and 5,801cells from old (Old 1: 1435, Old 2: 2,541, Old 3: 1,825).

tSNE analysis of single cell RNA-seq datasets and identification of cell clusters

To analyze the single cell RNA-seq data, we performed t-distributed stochastic neighbor embedding clustering using the Seurat R Package (version 2.3.4) (tSNE) with the first 15 principal components[55], after performing principal component analysis (PCA) on the 4,125 most variable genes. Identification of significant clusters was performed using the FindClusters() algorithm in the Seurat package which uses a shared nearest neighbor (SNN) modularity optimization based clustering algorithm[55]. Marker genes for each significant clusters were found using the Seurat function FindAllMarkers(). Cell types were determined

using a combination of marker genes identified from the literature and gene ontology for cell types using the web based tool Enrichr. (http://amp.pharm.mssm.edu/Enrichr/). This analysis identified 11 clusters of cells: astrocytes/qNSCs, aNSCs/NPCs, neuroblasts, neurons, OPCs, oligodendrocytes, endothelial cells, 'mural' cells (e.g. pericytes, smooth muscle), microglia, macrophages, and T cells. We note that ependymal cells, a known component of the NSC niche[56,57], were not identified, probably because these cells were too big to be uploaded in droplets, or were sheared in the 10x microfluidic device. In addition, we note that quantification of single cell data could be also influenced by different dissociation properties with age.

Clustering, heat maps, and violin plots for gene expression in single cells

Hierarchical clustering and heat map generation were performed for single cells on the basis of log-normalized (with scale factor 10,000 and pseudocount 1) expression values of marker genes curated from literature or identified as highly differentially expressed. Heat maps were generated using the heatmap.2 function from the gplots v3.0.1 R package using the default complete-linkage clustering algorithm. To visualize the expression of individual genes, cells were grouped by their cell type as determined by analysis with Seurat. Log-normalized gene expression values were plotted for each cell as a violin plot with an overlying dot plot in R.

Immunostaining of brain sections

All immunostainings were performed on C57BL/6 mice obtained from the NIA at the age indicated. Mice were subjected to intracardiac perfusion with 5mL of PBS containing heparin followed by 20mL of 4% paraformaldehyde in PBS. Brains were post-fixed for 24 hours in 4% paraformaldehyde. They were then subjected to dehydration in 30% sucrose. Brains were subsequently embedded in OCT and sectioned in 12μm coronal sections that were mounted on glass slides. To perform immunofluorescent staining, sections were first washed with PBS, followed by permeabilization with ice cold methanol with 0.2% Triton-X for 10 minutes at room temperature. Sections were blocked with 5% Normal Donkey Serum (ImmunoReagents Inc.) and 1% BSA (Fisher Biosciences) in PBS for 30 minutes at room temperature. Primary antibody staining was performed overnight at 4°C in 5% Normal Donkey Serum and 1% BSA in PBS. Primary antibodies used were the following: BST2 (BioLegend, Clone: 927, lot: B256699, [1:200]), CD3 (Novus Biological, Clone: SP7, lot: L139 and J275, [1:200], CD31 (R&D Systems, Product#:AF3628, lot: YZU0117021, [1:500]), IBA1 (Novus Biological, Product#: NB100–1028, lot: S7C7G2P24-E250517, [1:500], KI67 (eBioscience, Clone: SolA15, lot: 4328926, [1:500]), SOX2 (R&D Systems, Product#: AF2018, KOY0317071, [1:200]), STAT1 (Cell Signaling, Clone: D1K9Y, lot: 4 [1:500]). Sections were washed with PBS with 0.2% Tween and then with PBS only three times for 5 minutes at RT. Secondary antibody staining was performed at room temperature for 2 hours in 5% Normal Donkey Serum and 1% BSA in PBS. Secondary antibodies used were the following: donkey anti rabbit-AF568 (ThermoFisher [1:500]), donkey anti rat-AF488 (ThermoFisher [1:500]), donkey anti goat-AF647 (ThermoFisher [1:500]). Sections were washed with 0.2% Tween and then with PBS only three times for 5 minutes at RT. Sections were stained with DAPI at 1μg/mL for 10 minutes at RT. Sections were mounted with ProLong Gold (ThermoFisher) and visualized with a Nikon Eclipse Ti confocal microscope equipped with a Zyla sCMOS camera (Andor) and NIS-Elements software (AR

4.30.02, 64-bit) using the 20x, 60x or 100x objective. No blinding was done for picture taking. For visualization of images displayed in this manuscript, brightness and contrast were adjusted in Fiji to enhance visualization (these adjustments were not performed prior to the quantification described below). The same settings were applied to all images shown for each experiment.

Confocal microscopy image analysis and quantification

T cell and NSC quantification—The number of CD3+ T cells was manually counted in entire coronal sections of 5 young (3–7 months) and 4 old (20–24 months) male mice while directly visualizing each section under the microscope with the 20x objective. T cells were identified as CD3+DAPI+. Note that we observed the presence of T cells in various regions of old brains, not just the SVZ. The number of proliferative NSCs/NPCs (SOX2+KI67+) in the same sections and mice was counted manually while directly visualizing each section under the microscope with the 20x objective. NSCs/NPCs were identified as SOX2+KI67+DAPI+. The mean number of T cells or NSCs per coronal section was calculated for 4 sections total per mouse. Mean +/− s.e.m. was used for plotting and calculating *P*-values using the Wilcoxon rank-sum test.

STAT1 quantification—The entire SVZ area in both brain hemispheres was imaged using the 60x objective. Images were collected from five young (4–6 months) and four old (29–30 months) wildtype C57BL/6 male mice. Two brain sections were imaged per mouse. Fiji (ImageJ) was used for image analysis. Channels were split and image backgrounds were subtracted using a rolling ball radius chosen based on the size of the object being analyzed. A 50 pixel rolling ball radius was used for STAT1 and 100 pixel rolling ball radius was used for KI67 (a marker of cycling cells), SOX2 (a marker of the NSC lineage), IBA1 (a marker of microglia), and CD31 (a marker of endothelial cells). The same settings were applied to all experimental conditions. In SVZ sections from old mice, STAT1 colocalized with SOX2 (NSC lineage), IBA1 (microglia), and CD31 (endothelial cells). There was also colocalization between STAT1 and another NSC marker, glial fibrillary acidic protein (GFAP). The STAT1 fluorescence co-localizing with the cell marker of interest was quantified using a custom pipeline. Briefly, the channel for the cell type of interest (NSCs, microglia, or endothelial) was used to generate a mask by setting intensity thresholds to outline the positive areas. The same threshold values were used for all images across all conditions in each individual experiment. The cell masks were then used to determine the STAT1 fluorescence levels by mean intensity per masked pixel. The mean intensity STAT1 values were normalized for each independent experiment by dividing them by the median intensity of the young samples and the mean of these normalized values was used for plotting and calculating *P*-values using the Wilcoxon rank-sum test.

BST2 quantification in NSCs that are in proximity to T cells—Z-stacks of the entire SVZ area in both brain hemispheres were acquired with the 60x objective. The same exposure settings were used across all conditions in each individual experiment. Images were collected from three old (29–30 months) wildtype C57BL/6 male mice. Three brain sections were imaged per mouse. Fiji (ImageJ) was used for image analysis. For each image, the presence or absence of T cells was determined by the fluorescence intensity in the CD3

channel. When a T cell was detected, a rectangular area enclosing the T cell and the layers of NSCs lining the ventricle (defined by the SOX2 channel) was manually drawn. A region of the same dimensions was drawn when no T cell was present. The area of the box was kept the same for all samples analyzed. These areas were then used to determine the BST2 fluorescence levels by mean intensity across the Z-stack. The BST2 intensity was then averaged for each Z-stack. The mean intensity BST2 values were normalized for each independent experiment by dividing them by the median intensity of the 'No T cells' values. The *P*-value was calculated using the Wilcoxon rank-sum test. Note that BST2 staining was also observed in other cell types, including microglia, in SVZ sections from old mice (Extended Data Fig. 4g).

T cells in human brain specimens: selection, staining, and quantification

Human patient samples were obtained from the Stanford University Neuropathology Department. The Stanford autopsy brain bank, which contains brains from Stanford patients that have had autopsies with neuropathological examination, was searched over the last 20 years. First, cases that showed no significant neuropathological abnormalities were selected and classified by age. Cases that did not have appropriate tissue sections of the basal ganglia and cases where the medical history and other co-morbidities could have impact on the study were excluded. We excluded patients with neurological or significant neuropathological conditions, immune conditions (including leukemia, lymphoma, cytokine storm syndrome, severe hepatitis, immunodeficiency and autoimmune disease), ongoing or advanced cancer, recent chemo or radio therapy, recent transplants, or sepsis. Five young patients between 20 and 44 years and 6 older patients between 79 and 93 years of both sexes met the selection criteria and were included for the analysis (Supplementary Table 4).

Formalin-fixed paraffin-embedded brain tissues were sectioned at 5 μm thickness and histologic sections were stained with standard hematoxylin–eosin immunohistochemical staining (H&E). CD3 single-stain IHC was performed using anti-CD3 (Roche Ventana, 2GV6) antibody following the manufacturer's instruction on the Ventana Benchmark Ultra with EDTA pH 8.5 antigen retrieval. For CD8 single-stain IHC, anti-CD8 (Dako Aligent, C8/144B) was used following the manufacturer's instructions on the Leica Biosystem BOND-III Stainer with EDTA pH 9.0 antigen retrieval.

Brightfield images were taken with the 10x objective of an upright Zeiss AxioImager microscope equipped with a ZEISS Axiocam 503 mono camera and Zen Blue software. For each sample, the the subventricular zone, recognized by the ependymal lining, was imaged. For quantification of T cells, the images were analyzed using Fiji (ImageJ). The area lining the ventricle was calculated by drawing a box going 250 μm into the parenchyma. The number of CD3 or CD8 positive T cells within this area was then counted manually for each sample, excluding perivascular T cells, and expressed as the number of T cells per unit area (mm^2). *P*-values were calculated using the Wilcoxon rank-sum test.

CD8+ T cell isolation from blood, brain, and spleen.

For T cell isolation from aged brains, mice were sedated and perfused with 20mL of PBS with heparin sodium salt (Sigma Aldrich, 2mg/mL) to remove the blood. Brains were

immediately harvested thereafter. The SVZ was isolated as described above for "Single cell RNA-seq using the 10x Genomics Chromium single cell technology". Tissue dissociation when isolating pure populations of CD8+ T cells was carried out via a modified protocol from [58] using 2mg/mL collagenase type IV (Gibco) for 30 minutes at 37°C in HBSS with calcium and magnesium (Gibco), containing 14μg/mL of DNAse1 (Sigma Aldrich). The dissociated SVZ was then centrifuged through 22% Percoll (GE Healthcare) in PBS to remove myelin debris. Following centrifugation through Percoll solution, cells were washed with FACS buffer (HBSS, 1% BSA, 1% Glucose). Antibody staining was carried out in FACS buffer at the following dilutions: CD45-PE (Biolegend Cat.# 103105 Clone:30-F11 [1:100]), B220-PeCy5 (Biolegend Cat.# 103209 Clone: RA3–6B2 [1:100]), TER119-PeCy5 (Biolegend Cat.# 116209 Clone:TER-119 [1:100]), CD4-APC (Biolegend Cat.# 100411 Clone:GK1.5 [1:100]), CD8-FITC (Biolegend Cat.# 100705 Clone:53–6.7 [1:100]), CD11b-PerCP/Cy5.5 (Biolegend Cat.#101227 Clone:M1/70 [1:100]), CD3-AF700 (Biolegend Cat.#100216 Clone:17A2 [1:100]). Following primary antibody stain, cells were washed with FACS buffer and resuspended in FACS buffer containing 1μg/mL DAPI (ThermoFisher).

To isolate CD8+ T cells from blood, we collected blood samples through tail vein snip prior to perfusion. Approximately 50μL of blood was collected into 250μL of a 5U/mL solution of heparin sodium salt (Sigma-Aldrich), in PBS (Corning). Red blood cells were lysed by adding 2mL of ACK lysing buffer (ThermoFisher) for 10 minutes at RT. Following red blood cell lysis, 10mL of PBS was added to each tube and samples were spun for 10 minutes at 4°C. Samples were stained with an identical antibody panel as described above for isolation of CD8+ T cells from the brain.

To isolate CD8+ T cells from spleen, we removed the spleen and manually dissociated the tissue by chopping repeatedly with a scalpel blade. We then added the manually dissociated spleen to 2mL of ACK lysing buffer (ThermoFisher) to perform red blood cell lysis. Following red blood cell lysis, 10mL of PBS was added to each tube and samples were spun for 10 minutes at 4°C. Samples were stained with an identical antibody panel as described above for isolation of CD8+ T cells from the brain.

Smart-seq v4 single cell RNA-sequencing of purified brain and blood CD8+ T cells

To characterize T cells from old neurogenic niches, we generated single cell RNA-sequencing libraries from CD8+ T cells from the SVZ and blood of four old (25–29 months) male mice in two independent experiments, performed by two independent investigators (B.W.D. and M.T.B.) (Supplementary Table 7). We also generated libraries from the SVZ of two young (3 months) mice, though there were very few T cells in the SVZ of young mice (Supplementary Table 7). For library generation, we used the Clontech Smart-seq v4 kit to prepare cDNA. Briefly, CD8+ T cells, isolated as described above (defined as $CD45^{+}CD3^{+}CD4^{-}CD8^{+}B220^{-}TER119^{-}CD11b^{-}$) were clonally sorted into 5 μL of Clontech lysis buffer containing a 1:10,000,000 dilution of ERCC Mix1 (Ambion). cDNA was generated using following manufacturer's recommendations, as described in the manual (http://www.clontech.com/GQ/Products/cDNA_Synthesis_and_Library_Construction/Next_Gen_Sequencing_Kits/Single_cell_RNA_Seq_Kits_for_mRNA_seq/

Single_Cell_RNA_Seq_v4). The only alteration that was made to the protocol was that the reactions were scaled to one-half of the recommended volumes. Following cDNA generation, cDNA concentrations were measured an AATI Fragment analyzer. 50–100pg of cDNA were used as input into the Nextera XT DNA Library Prep Kit (Illumina). Manufacturer's recommendations were followed for the Nextera XT kit, except that all reactions were scaled to one-half of the recommended volumes. Resulting libraries were purified using Agencourt AMPure XP (Beckman Coulter) beads using a 1.8x cleanup. Libraries were multiplexed and sequenced on an Illumina NextSeq-500 (400m), using 75bp paired-end reads.

Analysis of TCR from Smart-seq single cell RNA-seq

To test whether T cells from old SVZs were clonally expanded, and whether their T cell receptor repertoire was similar to that of old blood T cells, we analyzed the sequence of their T cell receptors (TCR). Paired T-cell receptors (TCRα and TCRβ) were reconstructed from CD8+ T-cell Smart-seq v4 full-transcript RNA-sequencing data using the TraCeR software tool v0.5.1 (https://github.com/teichlab/tracer), described in Stubbington et al (2016)[59]. Briefly, TraCeR maps full-length cDNA reads to all possible combinations of V and J sequences, followed by contig assembly to determine recombined TCR sequences. Productive TCR-α and TCR-β sequences were reconstructed for 199 and 205 of 262 T cells (including 247 old T cells), respectively. TraCeR was run in an Anaconda environment on a Linux-based computing cluster using one node with 16Gb RAM.

TCR and cytokine transcript amplification using nested PCR sequencing

We also used an independent approach, based on nested PCR sequencing, to sequence the TCR and analyze cytokine transcripts from T cells from the SVZ and blood of 2 old (24 months) mice and 2 young (3 months) mice (Supplementary Table 7). TCR sequencing was done according to previously established protocols[29]. All primers were designed to have a T_m of 70–72 °C (Tm = 4×[GC]+2[AT]). All mouse TCR primer sequences are provided in Supplementary Table 13. For TCR primers, base degeneracy was incorporated into the primers when necessary to account for TCR polymorphism and ensure amplification of all known functional Vα, Vβ, Cα and Cβ regions identified in the IMGT database (http://www.imgt.org/). V-region primers were designed to be at least 50 bases from the distal end to ensure inclusion of the entire CDR3 region. All TCR primers for the second reaction contain the common sequence CCAGGGTTTTCCCAGTCACGAC at the 5′end, which enables amplification with barcoding primers during the third reaction. After all reactions are performed, TCR primers amplify a segment of the TCR of approximately 250bp. The final product for sequencing is approximately 380bp. Phenotyping PCR primers were designed to span introns and amplify all major variants of the genes present in the NCBI database (http://www.ncbi.nlm.nih.gov). After the second reaction is performed, phenotyping primers amplify a gene segment of approximately 200bp, and the final sequencing product is approximately 350bp.

TCR analysis by nested PCR

TCR sequence from single T cells were obtained by a series of three nested PCR reactions, as described[29]. For all Phase of PCR reactions, HotStarTaq DNA polymerase (Qiagen,

203203) was used. Phase 1 PCR reaction was multiplex PCR with multiple Vα and Vβ region primers, Cα and Cβ region primers in a 16μL reaction. For the Phase 1 PCR reaction, the final concentration of each TCR V-region primer is 0.06μM, each C-region primer is 0.3μM. A 16-cycle first PCR reaction was done per manufacturer's instructions using the following cycling conditions: 95°C 15 min; 94°C 30 s, 62°C 1 min, 72°C 1 min × 16 cycles; 72°C 10 min; 4°C. Thereafter, a 1μL aliquot of the Phase 1 product was used as a template for 12μL Phase 2 PCR reaction. The following cycling conditions were used for Phase 2 PCR: 95°C 15 min; 94°C 30 s, 64°C 1 min, 72°C 1 min × 25 cycles, 72°C 5 min; 4°C. For the Phase 2 reaction, multiple internally nested TCRVα, TCRVβ, TCRCα and Cβ primers were used (V primers 0.6μM, C primers 0.3μM). The Phase 2 primers of TCR V-region contained a common 23-base sequence at the 5′ end to enable further amplification (during the Phase 3 reaction) with a common 23-base primer. 1μL aliquot of the Phase 2 PCR product was used as a template for the 14μL Phase 3 PCR reaction, which incorporates barcodes and enables sequencing on the Illumina MiSeq platform. For the Phase 3 PCR reaction, amplification was performed using a 5′ barcoding primer (0.05μM) containing the common 23-base sequence and a 3′ barcoding primer (0.05μM) containing sequence of a third internally nested Cα and/or Cβ primer, and Illumina Paired-End primers (0.5μM each). The following cycling conditions were used for Phase 2 PCR: 95°C 15 min; 94°C 30 s, 66°C 30 s, 72°C 1 min × 25 cycles, 72°C 5 min; 4°C. The final Phase 3 barcoding PCR reactions for TCRα and TCRβ were done separately. For the Phase 3 reaction, 0.5μM of the 3′ Cα barcoding primer and the 3′ Cβ barcoding primer were used. In addition to the common 23-base sequence at the 3′ end (that enables amplification of products from the second reaction) and a common 23-base sequence at the 5′ end (that enables amplification with Illumina Paired-End primers), each 5′ barcoding primer contains a unique 5-base barcode that specifies plate and a unique 5-base barcode that specifies row within the plate. These 5′ barcoding primers were added with a multichannel pipette to each of 12 wells within a row within a plate. In addition to the internally nested TCR C-region sequence and a common 23-base sequence at the 3′ end (that enables amplification with Illumina Paired-End primers), each 3′ barcoding primer contains a unique 5-nucleotide barcode that specifies column. These 3' barcoding primers were added with a multichannel pipette to each of eight wells within a column within all plates. After the Phase 3 PCR reaction, each PCR product should have a unique set of barcodes incorporated that specifies plate, row and column and have Illumina Paired-End sequences that enable sequencing on the Illumina MiSeq platform. The PCR products were combined at equal proportion by volume, run on a 1.2% agarose gel, and a band around 350 to 380 bp was excised and gel purified using a Qiaquick gel extraction kit (Qiagen, 28704). This purified product was then sequenced.

TCR sequencing data was analyzed as previously described[29]. Briefly, raw sequencing data were processed and demultiplexed using a custom software pipeline to separate reads from every well in every plate as per specified barcodes. All paired ends are assembled by finding a consensus of at least 100 bases in the middle of the read. The resulting paired-end reads are then assigned to wells according to barcode. Primer dimers are filtered out by establishing minimum length of 100 bases for each amplicon. A consensus sequence is obtained for each TCR gene. Because multiple TCR genes might be present in each well, our software establishes a cutoff of >95% sequence identity within a given well. All

sequences exceeding 95% sequence identity are assumed to derive from the same TCR gene and a consensus sequence is determined. The 95% cutoff conservatively ensures all sequences derived from the same transcript would be properly assigned, even given a PCR rate of 1/9,000 bases, and sequencing error rate up to 0.4%[60] TCR V, D and J segments were assigned by VDJFasta. For phenotyping transcripts, the number of reads containing a 95% match to the customized database of transcription factor and cytokine genes are scored.

Age-Associated Pathway enrichment analysis

To investigate broad signatures of aging in each SVZ cell type sequenced, pre-ranked Gene Set Enrichment Analysis (GSEA) was carried out using pathways provided in MSigDB Hallmarks v6.1. The analysis was executed using an R implementation of the Broad Institute's pre-ranked GSEA algorithm (fgsea)[61]. For each cell type, genes were ranked by decreasing MAST derived Z-scores[62] with positive Z-scores corresponding to enrichment in old cells.

Fluidigm C1 single cell RNA-seq of NSC lineage

We also generated Fluidigm C1 single cell RNA-seq libraries for the NSC lineage. For this experiment, two young (3–4 months) and two old (20–24 months) male C57BL/6 mice obtained from the NIA Aged Colony were euthanized, and brains were immediately harvested. As described in [4], the SVZ from each hemisphere was micro-dissected. The SVZ was dissociated with enzymatic digestion with papain for 10 min at a concentration of 14U/mL. The dissociated SVZ was then titrated in a solution containing 0.7 mg/mL ovomucoid (Sigma-Aldrich), and 0.5 mg/mL DNAseI (Sigma-Aldrich) in DMEM/F12. The dissociated SVZ was then centrifuged through 22% Percoll in PBS to remove myelin debris. Following centrifugation through Percoll solution, cells were washed with FACS buffer (HBSS, 1% BSA, 1% Glucose). Antibody staining was carried out in FACS buffer at the following dilutions: Prom1-Biotin (eBioscience Cat.#13–1331-80 [1:300]), CD24-PacBlue (eBioscience Cat.#48–0242-80 [1:400]), CD31-PE (eBioscience Cat.#12–0311-81 [1:50]), CD45-BV605 (Biolegend Cat.#103139 [1:100]), O4-APC (Miltenyi Cat.#130–099-211 [1:50]) for one hour at 4°C. Samples were washed with 5mL of FACS buffer. Secondary staining was performed using Strep-PECy7 (eBioscience Cat.#25–4517-82 [1:500]) in FACS buffer at 4°C. Samples were washed with 5mL of FACS buffer, and resuspended in media containing 1μg/mL propidium iodide (Biolegend). Sorting performed on a BD FACS Aria II sorter, using a 100μm nozzle at 13.1 PSI. Cell gates were defined as follows[64]:

NSC-lineage: PROM1^{+}CD31^{-}CD24^{-}CD45^{-}O4^{-}—Cells were sorted into catching media: DMEM/F12 with B27 (1:50), B27 supplement (ThermoFisher, no Vitamin A, 1:50), N2 supplement (ThermoFisher, 1:100), 15mM HEPES buffer, 0.6% glucose, Penicillin-Streptomycin-Glutamine (Life Technologies, 1:100), and Insulin-Transferrin-Selenium (Life Technologies, 1:1000). Cells were then spun down at 300xg at 4°C and resuspended in catching media at a concentration of 300 cells/μL.

A 300 cell/μL cell solution was mixed at a 7:3 ratio with the Fluidigm C1 Suspension reagent and this solution was loaded onto a small size (5–10μm) Fluidigm C1 Single-Cell Auto Prep chip for all *in vivo* single cells studied and medium size (10–17μm) Fluidigm C1

Single-Cell Auto Prep chip for *in vitro* cultured neurosphere derived single cells. Live/dead staining was performed using the Fluidigm Live/Dead Cell Staining Solution as described in the Fluidigm C1 mRNA seq protocol and imaged using a Leica DMI4000B microscope. Reverse transcription was performed directly on the chip using the SMARTer chemistry from Clontech, and PCR was also performed on the chip using the Advantage PCR kit (SMARTer Ultra Low RNA Kit for the Fluidigm C1, Clontech #634832). ERCC spike in Mix 1 was included in the lysis buffer at a dilution of 1:1E5 from stock. Resulting cDNA was transferred to a 96 well-plate and a subset of representative samples were analyzed by bioanalyzer. A quarter of the cDNA for each library was quantified using the Quant-iT PicoGreen dsDNA Assay Kit (ThermoFisher Cat.# P11496) and verified to be within a range of 0.1–0.5ng/μL (or diluted when necessary with the C1 DNA dilution buffer). Sequencing libraries were prepared directly in a 96-well plate using the Nextera XT Library Preparation Kit (Illumina Cat. # FC-131–1024). Each library was individually barcoded using the Nextera XT 96-Sample Index Kit (Illumina Cat. # FC-131–1002), and all 96 barcoded libraries from each chip were pooled into single multiplexed libraries. The DNA concentration of multiplexed libraries was measured using BioAnalyzer. These multiplexed libraries were sequenced using the Illumina MiSeq (Illumina) at a concentration of 2pM. Details can be found in Supplementary Table 9.

Reads from cells sequenced via the Fluidigm C1 platform were mapped to mm10 using STAR, and gene counts were generated using HTseq. Cells were excluded from analysis if they were dead on the chip or if fewer than 500 genes were detected in an individual cell.

Principal component analysis with IFNγ response genes

To test whether single cells exhibit heterogeneous gene expression signatures with respect to IFNγ response genes, individual PCA plots were generated for specific cell types using genes in the IFNγ Response Hallmark gene set from MsigDB (http://software.broadinstitute.org/gsea/msigdb) (Supplementary Table 8). Log-transformed and normalized counts for each of the genes in the IFNγ Response Hallmark gene set were extracted from the log-transformed normalized gene expression values as calculated by Seurat. A subset of these genes including *Stat1*, *Irf9*, *Ifit1*, and *Ifitm3* were verified to be upregulated in cultured NSCs in response to IFNγ by RT-qPCR, indicating that NSCs could exhibit a classic transcriptional response to IFNγ. A principal component analysis (PCA) was then performed with only the genes this pathway and old cells were visualized using the first two principal components.

Intracellular FACS for STAT1

To stain NSCs and endothelial cells for STAT1, a gene characteristic of the IFN response, the subventricular zone was isolated and dissociated as described above for “Single cell RNA-seq using the 10x Genomics Chromium single cell technology”. Cells in the neural stem cell lineage including quiescent NSCs, activated NSCs, and NPCs were sorted as a population defined as $PROM1^{+}CD31^{-}CD24^{-}CD45^{-}O4^{-}$, and endothelial cells were defined as $CD31^{+}CD45^{-}O4^{-}$. Each cell type was FACS-sorted into catching media: DMEM/F12 with B27 (1:50), B27 supplement (ThermoFisher, no Vitamin A, 1:50), N2 supplement (ThermoFisher, 1:100), 15mM HEPES buffer, 0.6% glucose, Penicillin-Streptomycin-

Glutamine (Life Technologies, 1:100), and Insulin-Transferrin-Selenium (Life Technologies, 1:1000). Cells were then centrifuged at 300xg for 5 minutes at 4°C. To perform intracellular FACS on the isolated neural stem cell lineage ($PROM1^+CD31^-CD24^-CD45^-O4^-$), cells were resuspended in FACS buffer (HBSS, 1% BSA, 1% Glucose), and 16% PFA (ThermoFisher Cat.#28906) was added drop-wise to the cell suspension to reach a 1.6% final concentration. Cells were fixed in PFA at room temperature for 10 min. Cells were spun down at 500xg for 5 minutes and washed two times with FACS buffer. Cells were permeabilized with ice-cold methanol at 4°C for 10 min. Cells were centrifuged at 500xg for 5 minutes and washed two times with FACS buffer. Cells were blocked with DAKO protein block (DAKO) for 30 min at RT. Cells were subsequently stained with primary antibodies for STAT1 (Cell Signaling, Clone: D1K9Y [1:100]), and KI67 (eBioscience, Clone: SolA15 [1:200]) in FACS buffer overnight at 4°C. Cells were washed three times with 500μL of FACS buffer. Cells were stained with secondary antibodies donkey anti-rat 488 (ThermoFisher [1:200]), and donkey anti rabbit-PE (ThermoFisher [1:200]) in FACS buffer for 1 hour at 4°C. Cells were washed three times with 0.5mL FACS buffer. Cells were ultimately resuspended in 100μL of FACS buffer containing 1μg/mL DAPI (ThermoFisher) and were analyzed on a BD LSRII. Cells were analyzed in FlowJo.

FACS purification with CD317 (BST2/Tetherin) antibody

The sub-ventricular zone was isolated and dissociated as described above for “Single cell RNA-seq using the 10x Genomics Chromium single cell technology”. In some cases, mice were given a 1mg/mouse dose of 5-ethynyl-2’-deoxyuridine (EdU) via intraperitoneal injection 4 hours prior to euthanasia. Antibody staining was carried out in FACS buffer at the following dilutions: PROM1-Biotin (eBioscience Cat.#13–1331-80 [1:300]), EGF-AlexaFluor 647 (Life Technologies Cat. #E35351 [1:300]), CD24-PacBlue (eBioscience Cat.#48–0242-80 [1:400]), CD31-PE (eBioscience Cat.#12–0311-81 [1:50]), CD45-BV605 (Biolegend Cat.#103139 [1:100]), Strep-PECy7 (eBioscience Cat.#25–4517-82 [1:500]), O4-PE (Miltenyi Cat.#130–099-211 [1:50]), CD317-FITC (Biolegend Cat.#127002 Clone:927 [1:50]) for one hour at 4°C. Samples were washed with 5mL of FACS buffer. Secondary staining was performed using Strep-PECy7 (eBioscience Cat.#25–4517-82 [1:500]) in FACS buffer at 4°C. Samples were washed with 5mL of FACS buffer, and resuspended in media containing 1μg/mL propidium iodide (Biolegend). Fluorescent-minus-one controls were used to set positive gates in each experiment. Cell populations were defined as follows:

qNSCs – $PROM1^+EGFR^-CD31^-CD24^-CD45^-O4^-$

aNSCs/NPCs – $PROM1^+EGFR^+CD31^-CD24^-CD45^-O4^-$

BST2-positive aNSCs/NPCs – $PROM1^+EGFR^+CD31^-CD24^-CD45^-O4^-CD317^+$

BST2-negative aNSCs/NPCs – $PROM1^+EGFR^+CD31^-CD24^-CD45^-O4^-CD317^-$

BST2-positive and BST2-negative aNSCs/NPCs were subjected to subsequent analyses including bulk RNA-sequencing, EdU cycle analysis, and STAT1 staining.

Bulk RNA-sequencing of BST2-positive and BST2-negative NSCs

We performed bulk RNA-sequencing on BST2-positive and BST2-negative aNSCs/NPCs (defined as $PROM1^+EGFR^+CD31^-CD24^-CD45^-O4^-$) from and 4 old (23 months) C57BL/6 male mice from the NIA aged colony. SVZs were harvested and dissociated as described above, and cells were stained as described above in "FACS with CD317 (BST2/Tetherin) antibody". Cell identities were defined as follows:

Old BST2-positive aNSCs/NPCs – $PROM1^+EGFR^+CD31^-CD24^-CD45^-O4^-CD317^+$

Old BST2-negative aNSCs/NPCs – $PROM1^+EGFR^+CD31^-CD24^-CD45^-O4^-CD317^-$

Young aNSCs/NPCs – $PROM1^+EGFR^+CD31^-CD24^-CD45^-O4^-$

Because the number of BST2-positive aNSCs/NPCs was low for each old mouse and variable between mice, BST2-positive and BST2-negative aNSCs/NPCs were sorted in groups of 5 repeatedly until the sample had been exhausted. This process was repeated for each sample derived from independent mice, resulting in matched numbers of BST2-positive and BST2-negative aNSCs/NPCs for each mouse, ranging between 35 and 80 cells per mouse.

To perform the RNA-sequencing, the Clontech Smart-seq v4 Ultra-Low Input RNA kit (Clontech) was used. Cells were sorted into lysis buffer, as described in the protocol for the kit, and a 1:200,000 dilution of ERCC spike-in mix #1 (Ambion) was added. cDNA was prepared as described by the manufacturer. Each cDNA library was analyzed via bioanalyzer on a High Sensitivity chip on an Agilent 2100 Bioanalyzer. To generate sequencing libraries, 0.15 ng of each cDNA library was used as input in the Nextera XT kit, following manufacturer's recommendations. Cells were indexed using the Nextera XT Index Kit v2 Set A, and were subsequently multiplexed and sequenced on Illumina NextSeq-500 (400m), using 75bp paired-end reads.

Reads from cells sequenced via the Fluidigm C1 platform were mapped to mm10 using STAR, and gene counts were generated using HTseq.

Pathway enrichment for BST2-positive and BST2-negative RNA-sequencing

Pathway enrichment was assessed using the GSEA v3.0 algorithm with MSigDB Hallmarks V6.1, similarly to was done for age-associated enrichment (see above). The only change was that the rank file was generated by sorting genes based on their Z-scores calculated from edgeR[63] differential expression analysis results with default settings. Genes with Z-scores equivalent to 0 were removed from the ranked list.

EdU analysis of BST2-positive and BST2-negative NSCs

For EdU cell cycle analysis, BST2-positive and BST2-negative aNSCs/NPCs (defined as $PROM1^+EGFR^+CD31^-CD24^-CD45^-O4^-$) were FACS-sorted into separate wells of a V-bottom 96-well plate containing 100μL of Neurobasal-A (ThermoFisher) media with B27-supplement (ThermoFisher) [1:50]. Cells were washed once with PBS and fixed with 300μL

of ice-cold methanol at 4°C for 10 minutes. Click-it chemistry was performed with the Click-iT EdU Alexa Fluor 488 Flow Cytometry Assay Kit (ThermoFisher) according to the manufacturer's instructions. Following click reaction, cells were washed once with 0.5 ml of FACS buffer, and subsequently stained with 1:100 KI67-PE antibody (eBioscience Cat.#12–5698-82, Clone: SolA15) in FACS buffer for one hour at 4°C. For measurement of intracellular STAT1, cells were simultaneously stained with STAT1 (Cell Signaling, Clone: D1K9Y [1:100]). Following primary antibody staining, cells were washed twice with 0.5ml of FACS buffer. For measurement of intracellular STAT1, cells were stained with 1:500 Donkey anti rabbit-AF568 (ThermoFisher [1:500]). Following secondary staining, samples were washed twice with 0.5mL of FACS buffer and resuspended in FACS buffer containing 2μg/mL Hoechst (Molecular Probes). Samples were analyzed on a BD LSRII. Compensation was performed with OneComp eBeads (eBioscience). Final quantification of percentage EdU+ was only performed on samples including >30 cells.

Myelin oligodendrocyte glycoprotein (MOG) injection

Myelin oligodendrocyte glycoprotein (MOG) injection was performed according to previously established protocol used for experimental autoimmune encephalomyelitis[64]. Briefly, young male C57BL/6 mice (3 months old) from Jackson Laboratory were injected subcutaneously in the posterior right and left flank with an emulsion containing 200μg of MOG (Genemed synthesis Inc, MOG3555-P2–1) and an equal volume of complete Freund's adjuvant (CFA; Sigma-Aldrich, F5881) supplemented with 200μg of Mycobacterium tuberculosis H37Ra (Difco Laboratories, 231141). On the day of immunization and 2 days post-immunization, each mouse received 200ng of Pertussis toxin (PTX) (List Biological Laboratories, 180) as an adjuvant by intraperitoneal injection. On day 13–15 post-immunization, when mice were exhibiting early symptoms of hindlimb paralysis, the mice were sacrificed. In one experiment (MOG Experiment 1 – Supplementary Table 12), to assess T cell infiltration into the SVZ, the mice were sedated and perfused with 20 ml of PBS with heparin sodium salt (50 U/mL) (Sigma Aldrich) to remove the blood, and brains were immediately harvested. In the remaining MOG experiments (2, 3, 4, and 5), mice were sacrificed without perfusion, and the brains were harvested. In all experiments, SVZs were micro-dissected as described above. In MOG Experiment 1 (Supplementary Table 12), the SVZ was dissected from bilateral hemispheres, the SVZ from one hemisphere was enzymatically processed as described in "CD8+ T cell isolation from blood, brain, and spleen" to assess CD4+ and CD8+ T Cell infiltration, and the SVZ from the other hemisphere was processed as described in "FACS purification with CD317 (BST2/Tetherin) antibody", and stained and analyzed as described for the remaining MOG experiments described below. T cell FACS analysis was performed as described in "CD8+ T cell isolation from blood, brain, and spleen". For the remaining MOG experiments (MOG Experiment 2, 3, 4, and 5, Supplementary Table 12), the samples were processed as described in "FACS purification with CD317 (BST2/Tetherin) antibody" to assess BST2 status on aNSCs/NPCs. Cell gates for BST2-positive and -negative aNSCs/NPCs were defined as described in "FACS purification with CD317 (BST2/Tetherin) antibody". In MOG Experiment 4, to perform KI67 cell cycle analysis BST2-positive and BST2-negative aNSCs/NPCs (defined as $PROM1^{+}EGFR^{+}CD31^{-}CD24^{-}CD45^{-}O4^{-}$) (Extended Data Fig. 7) were FACS-sorted into separate wells of a V-bottom 96-well plate containing 100μL of Neurobasal-A

(ThermoFisher) media with B27 supplement (ThermoFisher) [1:50]. Cells were washed once with PBS and fixed with 300μL of ice-cold methanol at 4°C for 10 minutes. Cells were subsequently washed once with 0.5ml of FACS buffer, and subsequently stained with 1:100 KI67-PE antibody (eBioscience Cat.#12–5698-82, Clone: SolA15) in FACS buffer for one hour at 4°C. Samples were washed twice with 0.5mL of FACS buffer and resuspended in FACS buffer containing 2μg/mL Hoechst (Molecular Probes). Samples were analyzed on a BD LSRII. Final quantification of percentage KI67+ was only performed on samples including >30 cells.

Primary cultures of NSCs

To obtain primary cultures of young adult NSCs, the microdissected SVZ from C57BL/6 young male mice (3 months) from Jackson Laboratory was dissociated with enzymatic digestion with papain for 10 min at a concentration of 14U/mL. The dissociated SVZ was then titrated in a solution containing 0.7mg/mL ovomucoid (Sigma-Aldrich), and 0.5 mg/mL DNAseI (Sigma-Aldrich) in DMEM/F12. The dissociated SVZ was then centrifuged through 22% Percoll in PBS to remove myelin debris. Following centrifugation through Percoll solution, cells were washed with Neurobasal-A (ThermoFisher) supplemented with B27-supplement (ThermoFisher, no Vitamin A, 1:50). Cells were then resuspended in neurospheres cultures and maintained in Neurobasal-A (ThermoFisher) supplemented with B27-supplement (ThermoFisher, no Vitamin A, 1:50), Penicillin-Streptomycin-Glutamine (Life Technologies, 1:100), 20ng/mL of EGF (Peprotech), 20ng/mL of bFGF (Peprotech). To passage cells, they are dissociated for 5 minutes in Accutase (EMD Millipore) at 37°C and washed once in PBS (ThermoFisher), before resuspending the cells in growth media. To passage neurospheres, neurospheres were spun down at 300xg for 5 minutes, and then dissociated by resuspending and incubating for 5 minutes in 1mL of Accutase (EMD Millipore). Following incubation with Accutase, cells were and washed once in 10mL PBS (ThermoFisher). Cells were then resuspended and plated in Neurobasal-A (ThermoFisher) supplemented with B27-supplement (ThermoFisher, no Vitamin A, 1:50), Penicillin-Streptomycin-Glutamine (Life Technologies, 1:100), 20ng/mL of EGF (Peprotech), 20ng/mL of bFGF (Peprotech).

Primary co-cultures of T cell and NSCs

For primary co-cultures of T cell and NSCs, NSCs were isolated as described above. Early passage (P3) neurospheres were dissociated and plated at a density of 10,000 cells per well adherently onto 24 well plates, some containing 12mm round glass coverslips for immunofluorescence, coated overnight at 37°C with 20μg/mL Poly-D-Lysine (Sigma Aldrich) in PBS. Cells were grown for 48 hours adherently.

To get the high cell number needed for co-cultures, CD8+ T cells were freshly isolated from the spleen of a 3-month old male C57BL/6 mouse obtained from Jackson Laboratory. Briefly, the spleen was removed and a small piece of the apex of the spleen was removed and dissociated mechanically by chopping numerous times with a scalpel. The resulting tissue was subjected to red blood cell lysis using 2mL of ACK lysing buffer (ThermoFisher) at room temperature for 10 minutes. Cells were washed with 10mL of PBS. They were subsequently resuspended in FACS buffer (HBSS, 1% BSA, 0.1% Glucose) and filtered

through a 35μm snap cap filter (Corning). Antibody staining was carried out in FACS buffer at the following dilutions: CD45-PE (Biolegend Cat.# 103105 Clone:30-F11 [1:100]), B220-PeCy5 (Biolegend Cat.# 103209 Clone: RA3–6B2 [1:100]), TER119-PeCy5 (Biolegend Cat.# 116209 Clone:TER-119 [1:100]), CD4-APC (Biolegend Cat.# 100411 Clone:GK1.5 [1:100]), CD8-FITC (Biolegend Cat.# 100705 Clone:53–6.7 [1:100]), CD11b-PerCP/Cy5.5 (Biolegend Cat.#101227 Clone:M1/70 [1:100]), CD3-AF700 (Biolegend Cat.#100216 Clone:17A2 [1:100]). Following primary antibody stain cells were washed with FACS buffer and resuspended in FACS buffer containing 1μg/mL DAPI (ThermoFisher). CD8+ T cells (defined as $CD45^+CD3^+CD4^-CD8^+B220^-TER119^-CD11b^-$) were sorted into 5mL of Neurobasal-A media + 1:50 B27 supplement. T cells were spun at 300xg for 5 minutes and resuspended in 1mL of Neurobasal-A media.

Prior to adding T cells to NSC cultures, the media was changed in each well of NSCs to the media used to activate T cells. Two approaches were used to achieve T cell activation: 1) The combination of 5ng/mL IL2 (Carrier Free, R&D Systems), and 2μL of CD3/CD28 Dynabeads (Invitrogen) per well of a 24 well plate; or 2) The combination of 5ng/mL IL2 (Carrier Free, R&D Systems), 20ng/mL IL12 (Carrier Free, R&D Systems), 20ng/mL IL18 (Carrier Free, R&D Systems). All components were added to Neurobasal-A (ThermoFisher) supplemented with B27-supplement (ThermoFisher, no Vitamin A, 1:50), Penicillin-Streptomycin-Glutamine (Life Technologies, 1:100), 20ng/mL of EGF (Peprotech), 20ng/mL of bFGF (Peprotech). When indicated, either 10μg/mL anti-IFNγ antibody (Clone R4–6A2 BioXCell), or 10μg/mL Rat IgG1 Isotype control (Clone TNP6A7 BioXCell) were included.

For analysis of NSCs upon co-culture with T cells, 2,000 T cells were added to each well of NSCs and the plates were spun at 300xg for 5 minutes to sediment T cells on NSC cultures. T cell and NSC co-cultures were left undisturbed for 72 hours. After 72 hours, cells were incubated with 10μM 5-ethynyl-2'-deoxyuridine (EdU) for 4 hours. For FACS analysis, the cells were detached from the plate by removing the media and adding 200μL of Accutase (EMD-Millipore) to each well and incubating at 37°C for 5 minutes. Subsequently, cells were split evenly into two tubes. Half of the cells were spun down, washed once with FACS buffer (HBSS, 1% BSA, 1% Glucose), and subsequently stained with CD3-AF700 (Biolegend Cat.#100216 Clone:17A2 [1:100]) and CD317-FITC (Biolegend Cat.#127002 Clone:927 [1:50]) at 4°C for one hour. Each tube was washed with 0.5mL of FACS buffer, spun at 300xg for 5 minutes, and resuspended in 1μg/mL DAPI (ThermoFisher) in FACS buffer. The cells were analyzed live on an LSRII, excluding DAPI positive dead cells. Very few T cells were observed in these sorts, even in stimulated conditions, likely because they did not adhere well to the plates, and were aspirated away, and because they did not grow well in the NSC media. Thus, the vast majority of surviving cells were NSCs. The other half of the cells were spun down and fixed with 300μL of ice-cold 100% methanol at 4°C for 10 minutes. They were subsequently washed with 600μL of FACS buffer. Click-it chemistry was performed with the Click-iT EdU Alexa Fluor 488 Flow Cytometry Assay Kit (ThermoFisher) according to the manufacturer's instructions. Following click reaction, cells were washed once with 0.5 ml of FACS buffer, and subsequently stained with 1:100 Ki67-PE antibody (eBioscience Cat.#12–5698-82, Clone: SolA15) in FACS buffer for one hour at 4°C. Following antibody staining samples were washed twice with 0.5mL of FACS buffer

and finally resuspended in FACS buffer containing 2μg/mL Hoechst (Molecular Probes). Samples were analyzed on a BD LSRII. Compensation was performed with OneComp eBeads (eBioscience). All FACS data analysis was performed in FlowJo.

For immunofluorescence, cells were fixed in 4% PFA in PBS for 15 minutes at RT, followed by permeabilization in 0.2% (v/v) Tween-20 in PBS for 10 minutes at RT. Click-it chemistry was performed with the Click-iT Plus EdU Alexa Fluor 594 Imaging Kit (ThermoFisher) according to the manufacturer's instructions. Following click reaction the cells were washed twice in PBS and were then blocked in 5% Normal Donkey Serum (ImmunoReagents Inc.) and 1% BSA (Fisher Biosciences) in PBS for 30 minutes at RT. Primary and secondary antibody stainings were performed in 5% Normal Donkey Serum and 1% BSA in PBS for one hour at RT. Primary antibodies used were the following: BST2 (Biolegend, Clone: 927, [1:200]) and CD3 (Novus Biological, Clone: SP7 [1:200]). The cells were washed three times in blocking buffer after primary antibody staining and twice in blocking buffer, three times in 0.1% Tween-20 in PBS and three times in PBS only after secondary antibody incubation. The coverslips were mounted with ProLong Gold antifade reagent with DAPI (Invitrogen) and imaged with a Nikon Eclipse Ti confocal microscope equipped with a Zyla sCMOS camera (Andor) and NIS-Elements software (AR 4.30.02, 64-bit) using the 60x objective.

Statistical analyses

For most experiments, young and old mice/sample were processed in an alternate manner rather than in two large groups, to minimize group effect. While we did not do a *bona fide* power analysis, we took into account previous experiments to determine the number of animals needed in each experiment. For experiments, all tests were two-sided Wilcoxon rank sum tests. Results from individual experiments and statistical analysis are included in Supplementary Table 12.

Data Availability

All raw sequencing reads for single cell RNA-seq data (10x Genomics, Smart-seq v4, and Fluidigm C1) as well as bulk RNA-seq data can be found under BioProject PRJNA450425. The command and configuration files, in addition to a list of all versioned dependencies present in the running environment, are available on the Github repository for this paper (https://github.com/gitbuckley/SingleCellAgingSVZ).

Extended Data

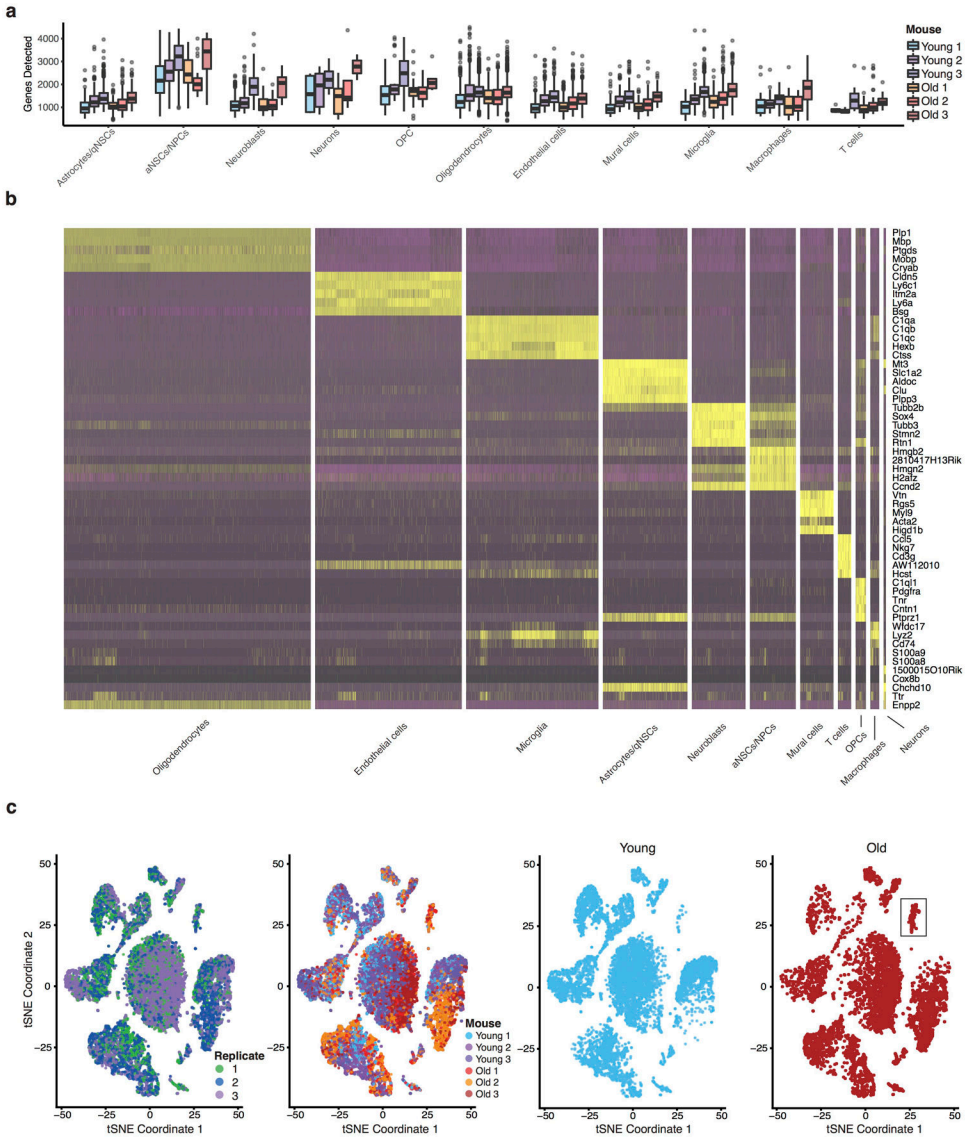

Extended Data Figure 1. Quality control for 10x Genomics single cell RNA-seq data.

a) Unique gene counts for 14,685 cells, separated by cell type and individual mouse (complete cell count breakdown available in Supplementary Table 3). Mean +/− 25th and 75th percentile are shown. Upper and lower whisker extend to 1.5x of the interquartile range; **b)** Heatmap showing the expression of the top 5 marker genes for each significant cell cluster identified by Seurat. The cell identity assigned to each cluster is indicated on the bottom of each column; **c)** t-SNE plots of all 14,685 10x Genomics single cell transcriptomes, colored by replicates, individual mouse, and separated by age. Clustering was the same as for Fig. 1a. 8,884 cells from young (Young 1: 2,306, Young 2: 2,675, Young 3: 3,903) and 5,801 cells from old (Old 1: 1435, Old 2: 2,541, Old 3: 1,825).

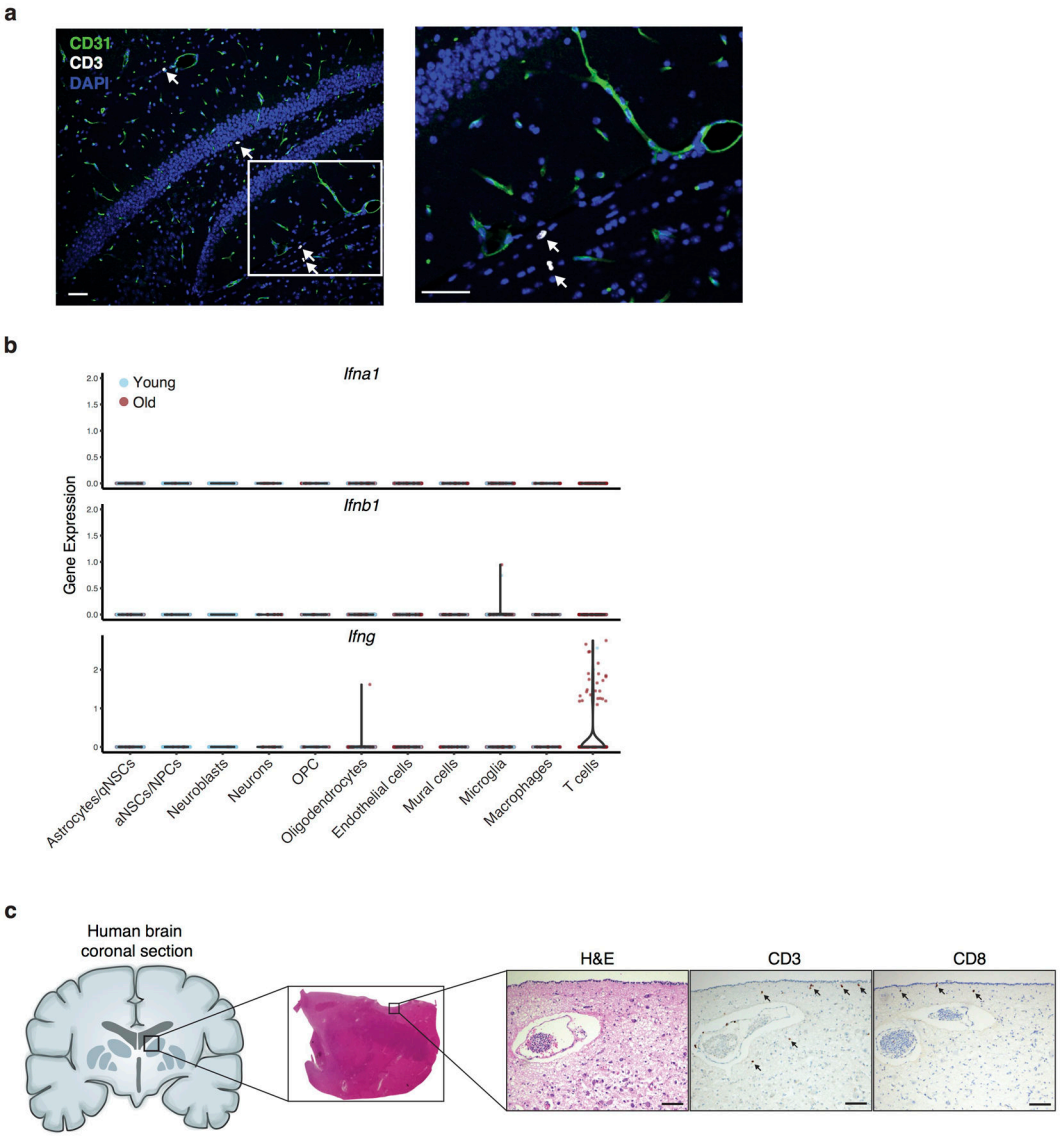

Extended Data Figure 2. T cells in old brains are within the brain parenchyma and express *Ifng*.

a) Immunofluorescence staining of brain sections of the SVZ neurogenic niche from old (24 months) male mice shows that age-associated T cells do not co-localize with markers of endothelial cells (CD31). Representative of n=4 old mice showing similar results. White: CD3 (T cells); Green: CD31 (endothelial cells); Blue: DAPI (DNA). The image on the right is from the white square. White arrows point at T cells. Scale bar: 50 μm; **b)** Violin plots showing expression of *Ifna1* (encoding IFNα), *Ifnb1* (encoding IFNβ) and *Ifng* (encoding IFNγ) in single cells from different cell types. The data for *Ifng* are also presented in Fig. 1h. Cell types were defined by cell clustering as defined in Fig. 1a. Cells were colored by age as in Fig. 1b. Expression values represented as normalized log2-transformed counts; **c)** Schematic of the experimental design for quantifying T cell infiltration in old human brains. Formalin-fixed paraffin-embedded brain tissue blocks of the basal ganglia with an identifiable ependymal lining (left and middle) from young and old humans were sectioned

and stained with H&E or antibodies to CD3 or CD8 for T cell quantification (right). Scale bars: 100 μm.

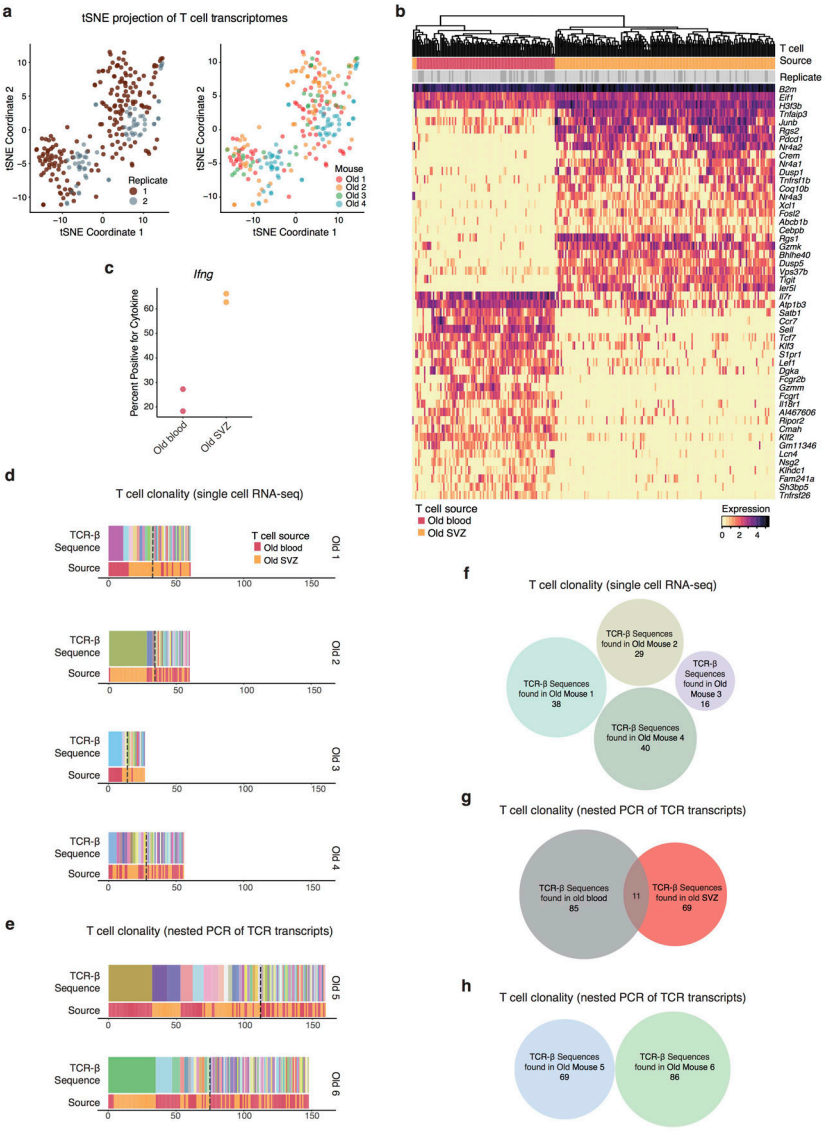

Extended Data Figure 3. T cells infiltrating old brains are clonally expanded and differ from T cells in old blood.

a) t-SNE projections of 247 CD8+ T cell transcriptomes from old blood and old SVZ (as in Fig. 2a), colored by experimental replicate and individual mouse; **b)** Expression of the top 50 differentially expressed genes upregulated for 247 CD8+ T cells isolated from old blood or old brain (SVZ) of old mice. Heat map of log-normalized counts, with single cells clustered by the expression of the genes shown in the plot. **c)** Expression of *Ifng* in T cells from blood or brains (SVZs) of 2 old (24 months) mice, as measured by nested PCR. Mean +/− s.e.m. of percent of T cells positive for *Ifng*. Nested PCR does not provide a quantitative metric but rather a binary determination of whether the T cell expresses the transcript for the cytokine or not. Percent of cells isolated from the SVZ or blood expressing *Ifng* is shown; **d, e)** Clonality of T cells isolated from the blood and perfused brain of old mice represented with the same X axis to enable direct comparison of clone sizes from different mice (the data are the same as Fig. 2c, d). TCR sequences were extracted from single cell RNA-sequencing

data using TraCer (Old Mouse 1, 2, 3, and 4) (d) or by nested PCR of the TCR transcripts (Old Mouse 5 and 6) (e). For each mouse TCR-β sequence clones are ordered from left to right in order of decreasing frequency in the top row. The source of the T cell is indicated in the bottom row. **f)** Venn diagram showing lack of overlap between T cell clones from separate mice, for the four mice for which their TCR repertoire was analyzed by single cell RNA-seq via TraCeR. TCR-β sequences were used, and all unique sequences were only counted once; **g, h)** Venn diagram showing lack of overlap between T cell clones from the old blood and old SVZ (g) or separate mice (h), for the two mice whose TCR repertoire was analyzed by nested PCR. TCR-β sequences were used, and all unique sequences were only counted once.

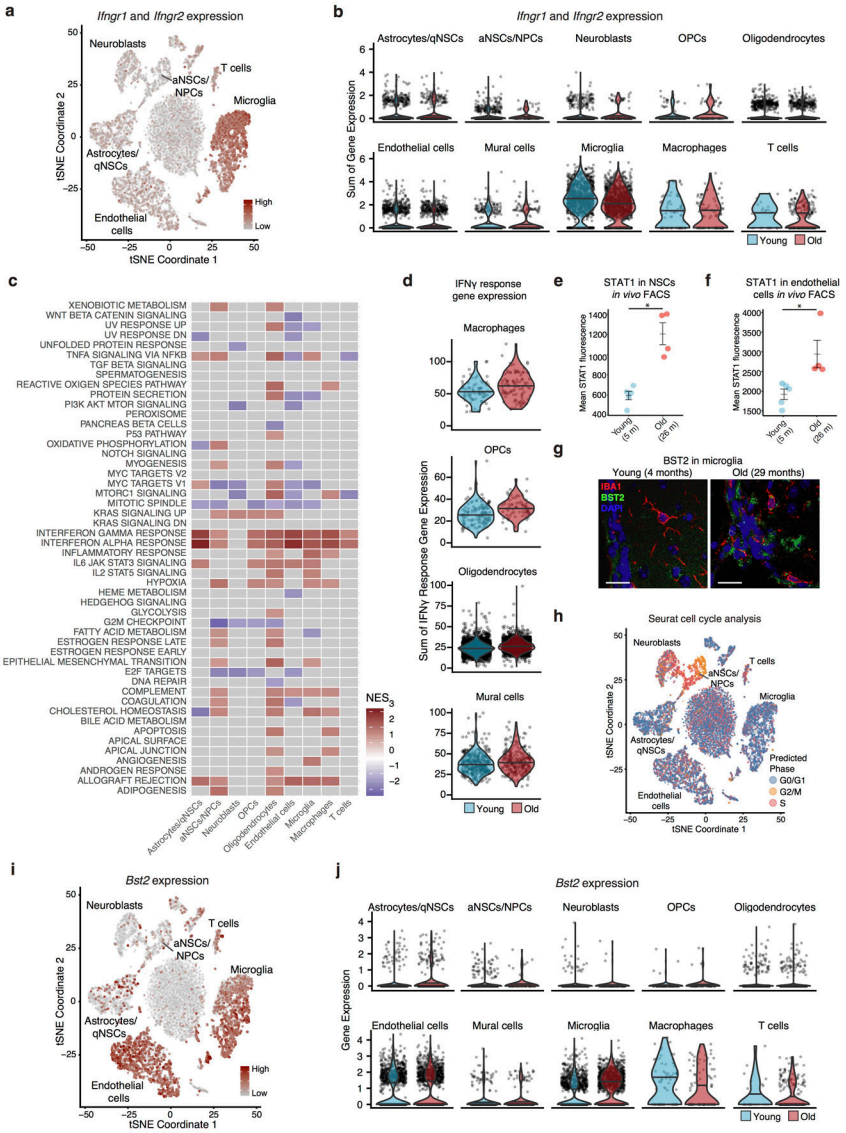

Extended Data Figure 4. The neurogenic niche responds to IFNγ.

a) t-SNE plot showing levels of expression of *Ifngr1* and *Ifngr2* (summed), which encode the IFNγ receptor, in 14,685 cells clustered as in Fig. 1a. Darker color indicates higher summed expression of *Ifngr1* and *Ifngr2*. Note that there is a lack of correlation between the age-dependent changes in *Ifngr1* and *Ifngr2* levels and changes in the IFNγ response (Fig. 3a), possibly because of post-transcriptional changes of the IFNγ receptor; **b)** Violin plots showing expression of *Ifngr1* and *Ifngr2* (summed) by age and cell type. Decrease in microglia is significant at $P<10^{-15}$ and others are not significant (n.s.), two-sided Wilcoxon rank sum test. Horizontal lines in violin plots denote median summed *Ifngr1* and *Ifngr2* expression. See Supplementary Table 3 for exact cell counts; **c)** MSigDB Hallmarks (v6.1) GSEA results for old versus young astrocytes/qNSCs, aNSCs/NPCs, Neuroblasts, OPCs, Oligodendrocytes, Endothelial cells, Microglia, Macrophages, and T cells in the neurogenic niche. Normalized enrichment score is presented for each pathway with *FDR*<0.05. Other cell types did not show pathways meeting this *FDR* cutoff; **d)** Combined log-normalized

expression values of genes in IFNγ Response Hallmark in various cell types of the SVZ. Single cells were grouped by cell type and age (Supplementary Table 3); **e)** FACS analysis of STAT1 levels in the young and old NSCs lineage (PROM1+CD45-CD31-CD24-O4-) freshly isolated from the brains of 5 young (5 months) and 4 old (26 months) male mice. Mean +/− s.e.m. of the mean STAT1 fluorescence of the ~500 cells analyzed for each mouse. Each dot represents ~500 cells from one mouse. *P=0.016, two-sided Wilcoxon rank sum test. Data from one experiment (all experiments are plotted in Extended Data Fig. 5d); **f)** FACS analysis of STAT1 levels in endothelial cells freshly isolated from the brains of 5 young (5 months) and 4 old (26 months) male mice. Mean +/− s.e.m. of the mean STAT1 fluorescence of the ~500 cells analyzed for each mouse. Each dot represents ~500 cells from one mouse. *P=0.016, two-sided Wilcoxon rank sum test; **g)** Immunofluorescence staining of SVZ brain sections from young (4 months) and old (29 months) male mice showing BST2 levels in microglia. Green: BST2; red: IBA1 (microglia maker); blue: DAPI. Scale bar: 20μm. **h)** t-SNE plot of 14,685 single cell transcriptomes with points colored by putative cell cycle phase (G0/G1, G2/M, or S) as predicted using Seurat's CellCycleScoring function; **i)** t-SNE plot of 14,685 single cell transcriptomes clustered as in Fig. 1a showing levels of expression of *Bst2* in cells of the subventricular zone (SVZ) neurogenic niche. Darker color indicates higher expression of *Bst2*; **j)** Violin plots showing *Bst2* expression by age and cell type. Horizontal lines in violin plots denote median *Bst2* expression. Increase in Astrocytes/qNSCs is significant at $P=6.4\times10^{-14}$, increase in Oligodendrocytes at P=0.025, increase in microglia at $P<2.2\times10^{-16}$, and others are not significant (n.s.), two-sided Wilcoxon rank sum test. See Supplementary Table 3 for exact cell counts.

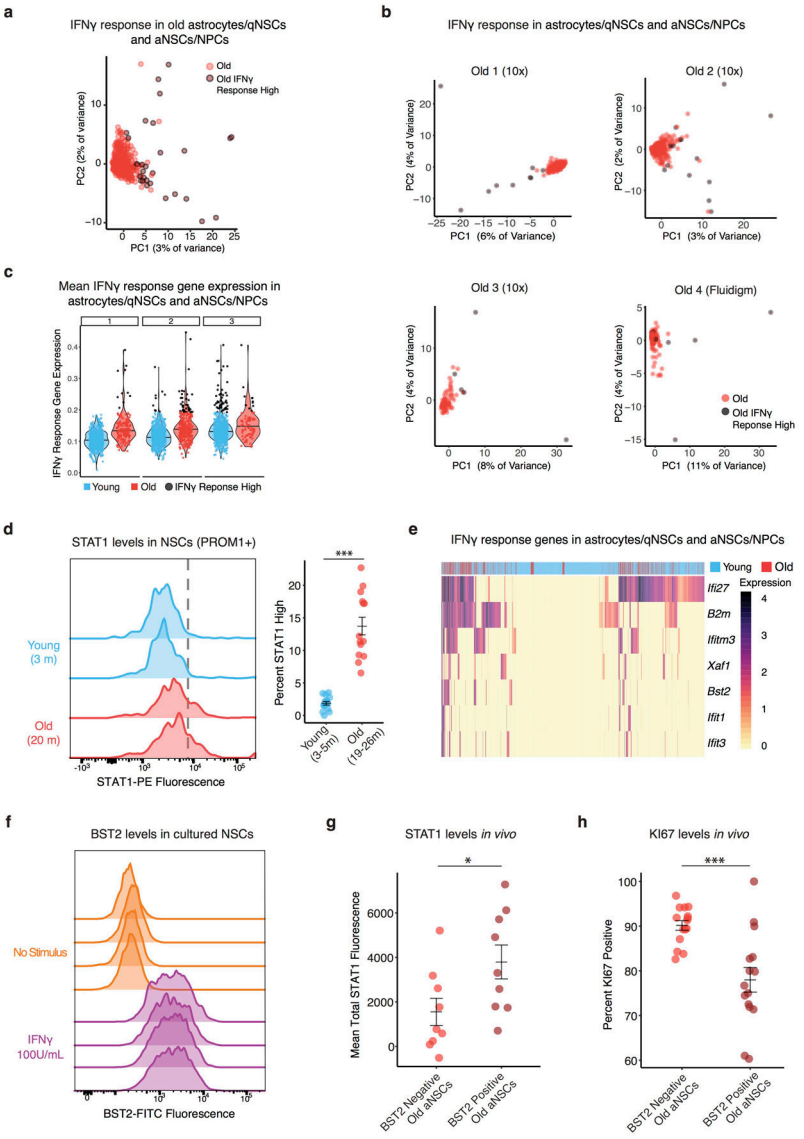

Extended Data Figure 5. The old NSC lineage exhibits a heterogeneous response to IFNγ.

a) Principal component analysis (PCA) of 562 old cells in the neural stem cell lineage (astrocytes/qNSCs and aNSCs/NPCs) performed only using genes in the IFNγ Response Hallmark from MSigDB (Supplementary Table 8). IFNγ-high cells (dark red with black ring) are defined as old cells exhibiting an average expression of genes in the IFNγ Response Hallmark pathway in the top 5% of old cells; **b)** PCA as in (a), but with a separate PCA performed for each of three 10x Genomics replicates (n=162, n=315, n=85 cells respectively) and for the dataset generated with Fluidigm C1 technology (n=137 cells); **c)** Average of normalized expression values of genes in IFNγ Response Hallmark for young and old cells in cells of the NSC lineage (Astrocytes/qNSCs and aNSCs/NPCs). Cells are grouped by age. IFN-high cells (in black) are defined as cells exhibiting an average expression of genes in the IFNγ Response Hallmark pathway in the top 5% of the cells analyzed within each 10x Genomics replicate. Note that replicate three contains ~2 fold more young cells than old cells. Horizontal lines in violin plots denote median IFNγ

Response Pathway expression. See Supplementary Table 3 for exact cell counts; **d)** FACS analysis of STAT1 positive cells in the young and old NSC lineage (PROM1+CD45−CD31−CD24−O4−). Left: FACS histograms of STAT1 fluorescence in PROM1+ cells isolated from the SVZ from two representative young (3 months) and old (20 months) male mice. Inset: Quantification of the percentage of STAT1-high cells in 15 young (3-5 months) and 14 old (19-26 months) mice. Mean +/− s.e.m. of percentage of cells that are STAT1-high of the ~500 cells analyzed for each mouse. Each dot represents ~500 cells from one mouse. The combined results from five independent experiments are shown (for independent experiments, see Supplementary Table 12). ***$P=5.08 \times 10^{-6}$, two-sided Wilcoxon rank sum test; **e)** The gene encoding the surface marker BST2/Tetherin is expressed in the old NSC lineage and is correlated with genes that belong to IFNγ signaling. Data is shown as heatmap with log-normalized expression of *Bst2* and other select genes in the IFNγ Response Hallmark pathway. Cells are clustered based on expression of this gene set. The age of the mouse from which the cells are isolated is indicated in a bar above the heatmap; **f)** Live FACS analysis for BST2 in cultured NSCs following IFNγ treatment for 48 hours; **g)** Abundance of total STAT1 protein in BST2-positive versus BST2-negative aNSCs/NPCs isolated from 9 old (25 months) mice, as measured by intracellular FACS. Mean +/− s.e.m. of total STAT1 fluorescence. Each dot represents cells from one mouse. The combined results from two independent experiments are shown (for independent experiments, see Supplementary Table 12). *$P=0.04$, two-sided Wilcoxon rank sum test; **h)** FACS quantification for KI67, a marker of cycling cells, in BST2-positive and BST2-negative aNSCs/NPCs from 15 old (23-25 months) mice. Mean +/− s.e.m. of percentage of cells that are KI67 positive of the ~100 cells analyzed for each mouse. Each dot represents ~100 cells from one mouse. The combined results from three independent experiments are shown (for independent experiments, see Supplementary Table 12). ***$P=7.80 \times 10^{-4}$, two-sided Wilcoxon rank sum test.

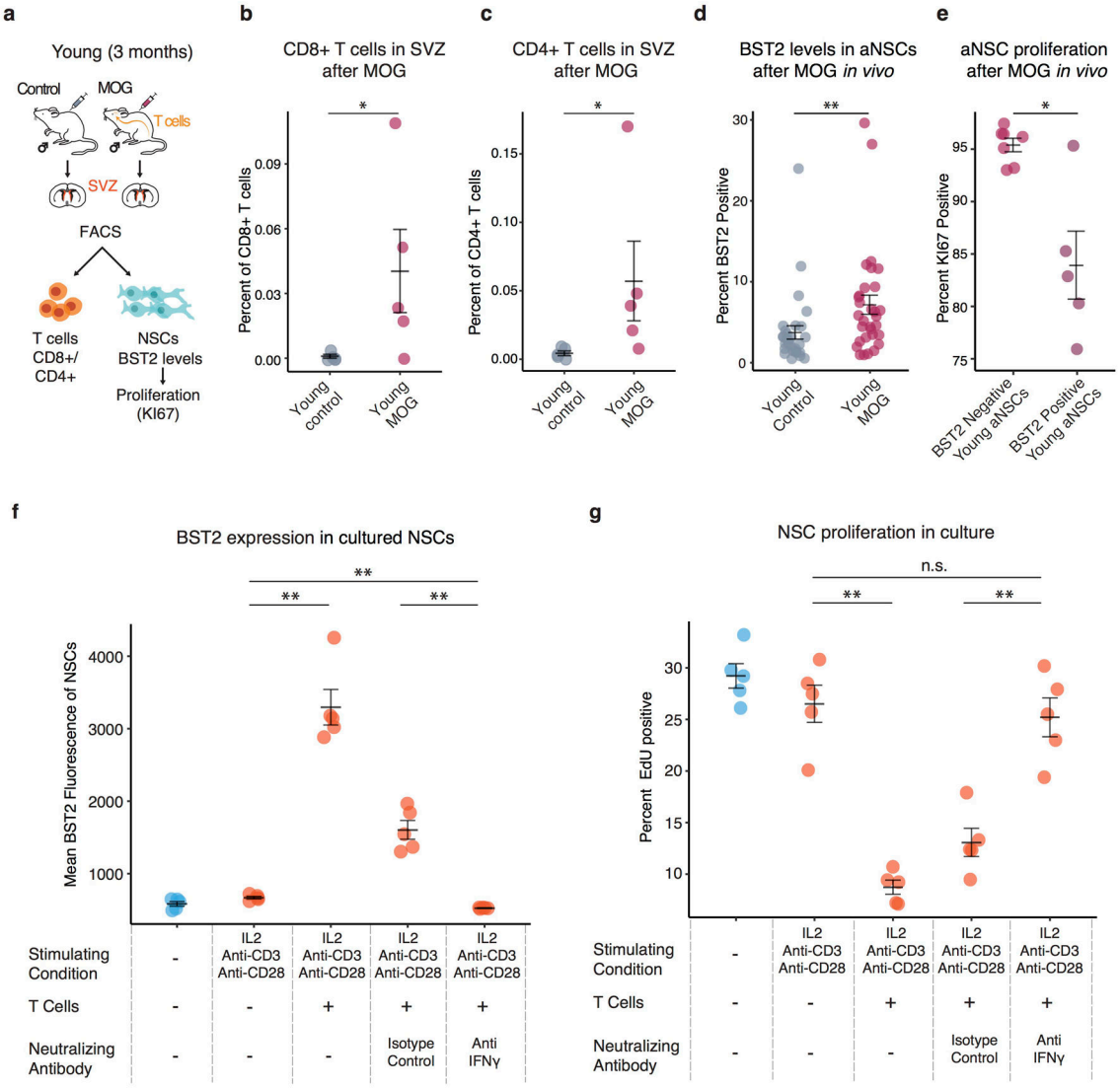

Extended Data Figure 6. T cells can influence NSCs *in vivo* and in co-cultures.

a) Schematic showing approach for inducing T cell infiltration of the brains of young mice by immunization with recombinant myelin oligodendrocyte glycoprotein (MOG). NSCs were purified 13-15 days after MOG immunization, and BST2 levels and proliferative (cycling) status (as determined by intracellular KI67 levels) of NSCs were measured by FACS; **b, c)** FACS analysis of CD8+ (b) and CD4+ (c) T cells freshly isolated from the brains of 5 control or 5 MOG-injected young mice (3 months). Mean +/− s.e.m of the percent of live cells that are defined as CD8+ or CD4+ T cells, defined as CD3+CD45+TCRγ/δ−B220−TER119−CD11b−. **P*=0.016 (b), **P*=0.045 (c), two-sided Wilcoxon rank sum test. Each dot represents one mouse; **d)** Percent of aNSCs/NPCs that are BST2-positive sorted from 30 young (3 months) male mice injected with adjuvant (control) and 31 young (3 months) male mice injected with adjuvant with MOG (See Experimental Procedures), combined over 5 experiments (for individual experiments, see Supplementary Table 12). Mean +/− s.e.m. of the percentage of cells that are BST2-positive of the ~500 cells analyzed from each mouse. Each dot represents cells from one mouse. ***P*=0.002, two-

sided Wilcoxon rank sum test. **e)** FACS analysis for KI67, a marker of cycling cells, in freshly isolated BST2-positive and BST2-negative aNSCs/NPCs sorted from 7 MOG-injected young mice (3 months). Mean +/− s.e.m. of the percentage of cells that are KI67-positive of the ~100 cells analyzed from each mouse. Samples were excluded if there were fewer than 30 intact cells analyzed in a given sample (resulting in 7 samples for BST2-negative and 5 samples for BST2-positive aNSCs/NPCs). Each dot represents cells from one mouse. **P*=0.018, Two-sided Wilcoxon rank sum test. **f, g)** BST2 levels (f) and EdU incorporation (g) in cultured NSCs following co-culture with spleen CD8+ T cells incubated with a combination of IL2, along with beads coated with anti-CD3 and anti-CD28 antibodies, which are known to activate CD8+ T cells. BST2 levels in NSCs, measured by live FACS analysis, plotted as mean BST2 fluorescence. Percent of NSCs incorporating EdU, a nucleotide analogue, during a 4-hour pulse of EdU. Effects of activated T cells on NSCs are reversed by the addition of a neutralizing antibody to IFNγ. Mean+/− s.e.m. of the percentage of cells that are BST2-positive or EdU-positive of the ~1,000 cells analyzed from each NSC culture. Each dot represents an independent culture of NSCs, derived from a separate mouse (n=5). One independent experiment (see Supplementary Table 12). ***P*=0.008, n.s.=not significant, two-sided Wilcoxon rank sum test.

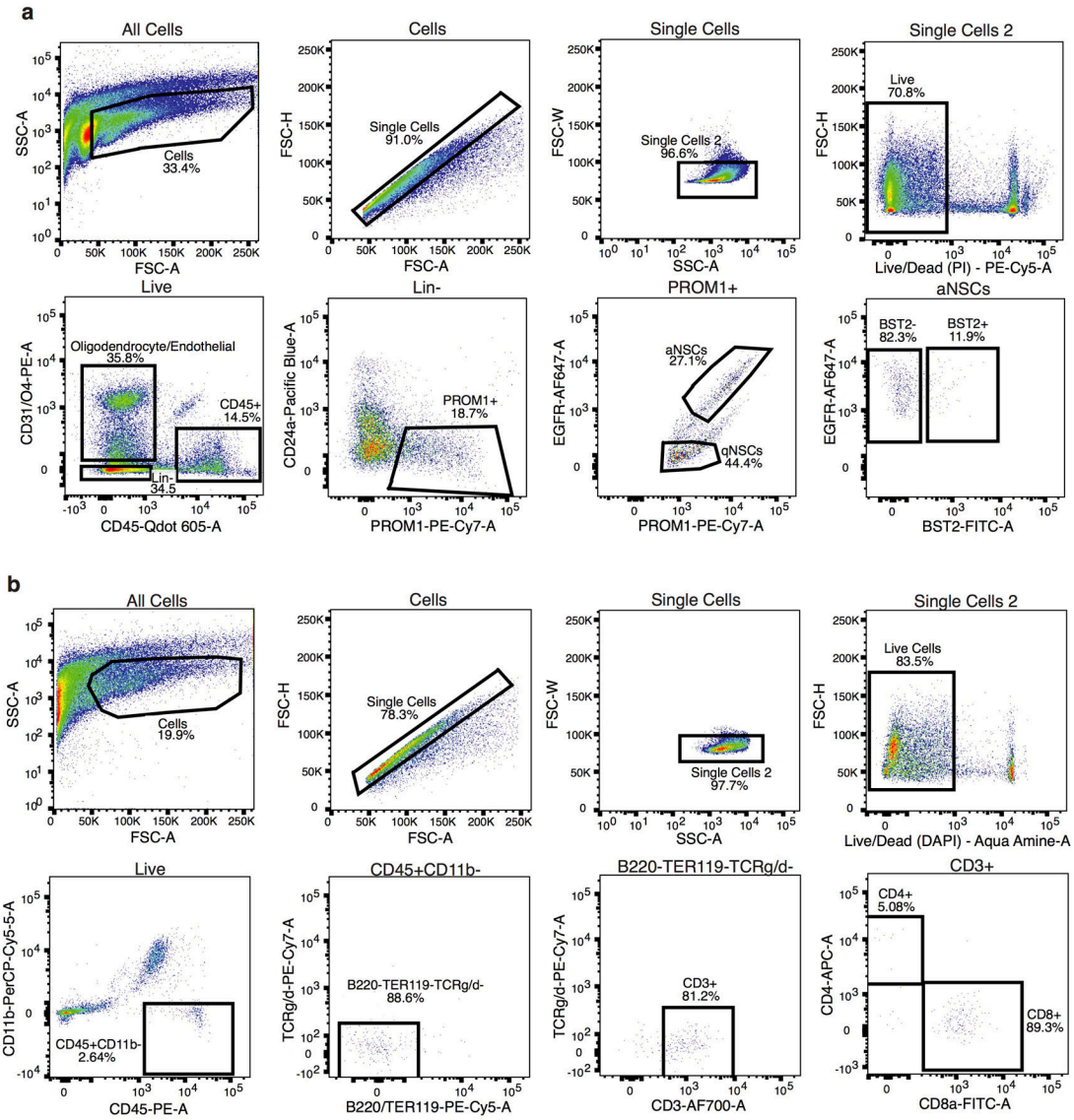

Extended Data Figure 7. FACS gating strategies.

a) FACS scheme for the isolation of PROM1+EGFR+CD45−CD31−O4−CD24a− aNSCs/NPCs from the adult SVZ. Gate shown on each plot is indicated above the plot. Marker and fluorophore are shown on each axis; **b)** FACS scheme for the isolation of CD8+CD4-CD3+CD45+TCRγ/δ−B220−TER119−CD11b− T cells from adult SVZ, spleen, and blood. Gate shown on each plot is indicated above the plot. Marker and fluorophore are shown on each axis.

Supplementary Material

Refer to Web version on PubMed Central for supplementary material.

Acknowledgements

We thank Dhananjay Wagh from the Stanford Functional Genomics Facility for assistance with 10x Genomics libraries and Fluidigm Corporation for help with Fluidigm C1 libraries. We thank the Stanford Shared FACS Facility and Cathy Carswell-Crumpton for FACS support. We thank Theo Palmer, Tom Rando, Anshul Kundaje, Michelle Monje-Deisseroth and Vittorio Sebastiano for guidance. Supported by NIH P01 AG036695 (A.B), a generous gift from Tim and Michele Barakett (A.B.), NIH T32 GM7365 (B.W.D.), Stanford MSTP program (B.W.D.), NSF Graduate Research Fellowship (M.T.B.), and Human Frontiers Science Program Long-term Fellowship (P.N.N).

References

1. Mirzadeh Z, Merkle FT, Soriano-Navarro M, Garcia-Verdugo JM & Alvarez-Buylla A Neural stem cells confer unique pinwheel architecture to the ventricular surface in neurogenic regions of the adult brain. Cell Stem Cell 3, 265–78 (2008). [PubMed: 18786414]
2. Shen Q et al. Adult SVZ stem cells lie in a vascular niche: a quantitative analysis of niche cell-cell interactions. Cell Stem Cell 3, 289–300 (2008). [PubMed: 18786416]
3. Tavazoie M et al. A specialized vascular niche for adult neural stem cells. Cell Stem Cell 3, 279–88 (2008). [PubMed: 18786415]
4. Codega P et al. Prospective identification and purification of quiescent adult neural stem cells from their in vivo niche. Neuron 82, 545–59 (2014). [PubMed: 24811379]
5. Bond AM, Ming GL & Song H Adult Mammalian Neural Stem Cells and Neurogenesis: Five Decades Later. Cell Stem Cell 17, 385–95 (2015). [PubMed: 26431181]
6. Gage FH & Temple S Neural stem cells: generating and regenerating the brain. Neuron 80, 588–601 (2013). [PubMed: 24183012]
7. Maslov AY, Barone TA, Plunkett RJ & Pruitt SC Neural Stem Cell Detection, Characterization, and Age-Related Changes in the Subventricular Zone of Mice. The Journal of Neuroscience 24, 1726–1733 (2004). [PubMed: 14973255]
8. Luo J, Daniels SB, Lennington JB, Notti RQ & Conover JC The aging neurogenic subventricular zone. Aging Cell 5, 139–52 (2006). [PubMed: 16626393]
9. Chaker Z, Aid S, Berry H & Holzenberger M Suppression of IGF-I signals in neural stem cells enhances neurogenesis and olfactory function during aging. Aging Cell 14, 847–56 (2015). [PubMed: 26219530]
10. Enwere E et al. Aging results in reduced epidermal growth factor receptor signaling, diminished olfactory neurogenesis, and deficits in fine olfactory discrimination. J Neurosci 24, 8354–65 (2004). [PubMed: 15385618]
11. Tropepe V, Craig CG, Morshead CM & van der Kooy D Transforming Growth Factor-α Null and Senescent Mice Show Decreased Neural Progenitor Cell Proliferation in the Forebrain Subependyma. The Journal of Neuroscience 17, 7850–7859 (1997). [PubMed: 9315905]
12. Molofsky AV et al. Increasing p16INK4a expression decreases forebrain progenitors and neurogenesis during ageing. Nature 443, 448–52 (2006). [PubMed: 16957738]
13. Ahlenius H, Visan V, Kokaia M, Lindvall O & Kokaia Z Neural Stem and Progenitor Cells Retain Their Potential for Proliferation and Differentiation into Functional Neurons Despite Lower Number in Aged Brain. The Journal of Neuroscience 29, 4408 (2009). [PubMed: 19357268]
14. Leeman DS et al. Lysosome activation clears aggregates and enhances quiescent neural stem cell activation during aging. Science 359, 1277–1283 (2018). [PubMed: 29590078]
15. Silva-Vargas V, Maldonado-Soto Angel R., Mizrak D, Codega P & Doetsch F Age-Dependent Niche Signals from the Choroid Plexus Regulate Adult Neural Stem Cells. Cell Stem Cell 19, 643–652 (2016). [PubMed: 27452173]
16. Ernst A et al. Neurogenesis in the striatum of the adult human brain. Cell 156, 1072–83 (2014). [PubMed: 24561062]
17. Llorens-Bobadilla E et al. Single-Cell Transcriptomics Reveals a Population of Dormant Neural Stem Cells that Become Activated upon Brain Injury. Cell Stem Cell 17, 329–340 (2015). [PubMed: 26235341]

18. Hochgerner H,.Z. Amit, Lönnerberg Peter, Linnarsson Sten Conservation of differentiation but transformation of initiation in hippocampal neurogenesis. Nat Neurosci 21, 290–299 (2018). [PubMed: 29335606]
19. Shin J et al. Single-Cell RNA-Seq with Waterfall Reveals Molecular Cascades underlying Adult Neurogenesis. Cell Stem Cell 17, 360–72 (2015). [PubMed: 26299571]
20. Dulken BW, Leeman DS, Boutet SC, Hebestreit K & Brunet A Single-Cell Transcriptomic Analysis Defines Heterogeneity and Transcriptional Dynamics in the Adult Neural Stem Cell Lineage. Cell Reports 18, 777–790 (2017). [PubMed: 28099854]
21. Luo Y et al. Single-cell transcriptome analyses reveal signals to activate dormant neural stem cells. Cell 161, 1175–86 (2015). [PubMed: 26000486]
22. Mizrak D et al. Single-Cell Analysis of Regional Differences in Adult V-SVZ Neural Stem Cell Lineages. Cell Rep 26, 394–406.e5 (2019). [PubMed: 30625322]
23. Zywitza V, Misios A, Bunatyan L, Willnow TE & Rajewsky N Single-Cell Transcriptomics Characterizes Cell Types in the Subventricular Zone and Uncovers Molecular Defects Impairing Adult Neurogenesis. Cell Rep 25, 2457–2469.e8 (2018). [PubMed: 30485812]
24. Basak O et al. Troy+ brain stem cells cycle through quiescence and regulate their number by sensing niche occupancy. Proc Natl Acad Sci U S A 115, E610–e619 (2018). [PubMed: 29311336]
25. Shi Z et al. Single-cell transcriptomics reveals gene signatures and alterations associated with aging in distinct neural stem/progenitor cell subpopulations. Protein & Cell 9, 351–364 (2018). [PubMed: 28748452]
26. Kalamakis G et al. Quiescence Modulates Stem Cell Maintenance and Regenerative Capacity in the Aging Brain. Cell 176, 1407–1419.e14 (2019). [PubMed: 30827680]
27. Haring JS, Badovinac VP & Harty JT Inflaming the CD8+ T cell response. Immunity 25, 19–29 (2006). [PubMed: 16860754]
28. Montagne A et al. Blood-Brain Barrier Breakdown in the Aging Human Hippocampus. Neuron 85, 296–302 (2015). [PubMed: 25611508]
29. Han A, Glanville J, Hansmann L & Davis MM Linking T-cell receptor sequence to functional phenotype at the single-cell level. Nat Biotechnol 32, 684–92 (2014). [PubMed: 24952902]
30. Schroder K, Hertzog PJ, Ravasi T & Hume DA Interferon-gamma: an overview of signals, mechanisms and functions. J Leukoc Biol 75, 163–89 (2004). [PubMed: 14525967]
31. Yu Q et al. Type I interferon controls propagation of long interspersed element-1. J Biol Chem 290, 10191–9 (2015). [PubMed: 25716322]
32. De Cecco M et al. L1 drives IFN in senescent cells and promotes age-associated inflammation. Nature 566, 73–78 (2019). [PubMed: 30728521]
33. Pereira L, Medina R, Baena M, Planas AM & Pozas E IFN gamma regulates proliferation and neuronal differentiation by STAT1 in adult SVZ niche. Frontiers in Cellular Neuroscience 9, 270 (2015). [PubMed: 26217191]
34. Baruch K et al. Aging. Aging-induced type I interferon response at the choroid plexus negatively affects brain function. Science 346, 89–93 (2014). [PubMed: 25147279]
35. Li L, Walker TL, Zhang Y, Mackay EW & Bartlett PF Endogenous interferon gamma directly regulates neural precursors in the non-inflammatory brain. J Neurosci 30, 9038–50 (2010). [PubMed: 20610738]
36. Filiano AJ et al. Unexpected role of interferon-γ in regulating neuronal connectivity and social behaviour. Nature 535, 425 (2016). [PubMed: 27409813]
37. Yoo H, Park SH, Ye SK & Kim M IFN-gamma-induced BST2 mediates monocyte adhesion to human endothelial cells. Cell Immunol 267, 23–9 (2011). [PubMed: 21094940]
38. Holmgren AM, Miller KD, Cavanaugh SE & Rall GF Bst2/Tetherin Is Induced in Neurons by Type I Interferon and Viral Infection but Is Dispensable for Protection against Neurotropic Viral Challenge. Journal of Virology 89, 11011–11018 (2015). [PubMed: 26311886]
39. Evans DT, Serra-Moreno R, Singh RK & Guatelli JC BST-2/tetherin: a new component of the innate immune response to enveloped viruses. Trends in microbiology 18, 388–396 (2010). [PubMed: 20688520]

40. Constantinescu CS, Farooqi N, O'Brien K & Gran B Experimental autoimmune encephalomyelitis (EAE) as a model for multiple sclerosis (MS). British journal of pharmacology 164, 1079–1106 (2011). [PubMed: 21371012]
41. Weiss HA, Millward JM & Owens T CD8+ T cells in inflammatory demyelinating disease. J Neuroimmunol 191, 79–85 (2007). [PubMed: 17920696]
42. Raue HP, Brien JD, Hammarlund E & Slifka MK Activation of virus-specific CD8+ T cells by lipopolysaccharide-induced IL-12 and IL-18. J Immunol 173, 6873–81 (2004). [PubMed: 15557182]
43. Town T, Tan J, Flavell RA & Mullan M T-cells in Alzheimer's disease. Neuromolecular Med 7, 255–64 (2005). [PubMed: 16247185]
44. Sulzer D et al. T cells from patients with Parkinson's disease recognize α-synuclein peptides. Nature 546, 656 (2017). [PubMed: 28636593]
45. Buckwalter MS et al. Increased T Cell Recruitment to the CNS after Amyloid Immunization in Alzheimer's Mice Overproducing Transforming Growth Factor-β1. The Journal of Neuroscience 26, 11437 (2006). [PubMed: 17079673]
46. Ritzel RM et al. Age-Associated Resident Memory CD8 T Cells in the Central Nervous System Are Primed To Potentiate Inflammation after Ischemic Brain Injury. The Journal of Immunology 196, 3318 (2016). [PubMed: 26962232]
47. Mrdjen D et al. High-Dimensional Single-Cell Mapping of Central Nervous System Immune Cells Reveals Distinct Myeloid Subsets in Health, Aging, and Disease. Immunity 48, 380–395 e6 (2018). [PubMed: 29426702]
48. Salter MW & Stevens B Microglia emerge as central players in brain disease. Nat Med 23, 1018–1027 (2017). [PubMed: 28886007]
49. Pober JS & Sessa WC Evolving functions of endothelial cells in inflammation. Nat Rev Immunol 7, 803–15 (2007). [PubMed: 17893694]
50. Kokaia Z, Martino G, Schwartz M & Lindvall O Cross-talk between neural stem cells and immune cells: the key to better brain repair? Nat Neurosci 15, 1078–87 (2012). [PubMed: 22837038]
51. Louveau A, Harris TH & Kipnis J Revisiting the Mechanisms of CNS Immune Privilege. Trends in immunology 36, 569–577 (2015). [PubMed: 26431936]
52. Ziv Y, Avidan H, Pluchino S, Martino G & Schwartz M Synergy between immune cells and adult neural stem/progenitor cells promotes functional recovery from spinal cord injury. Proceedings of the National Academy of Sciences 103, 13174–13179 (2006).
53. McGavern DB, Homann D & Oldstone MBA T Cells in the Central Nervous System: The Delicate Balance between Viral Clearance and Disease. The Journal of Infectious Diseases 186, S145–S151 (2002). [PubMed: 12424690]
54. Wakim LM, Woodward-Davis A & Bevan MJ Memory T cells persisting within the brain after local infection show functional adaptations to their tissue of residence. Proceedings of the National Academy of Sciences 107, 17872 (2010).
55. Satija R, Farrell JA, Gennert D, Schier AF & Regev A Spatial reconstruction of single-cell gene expression data. Nat Biotech 33, 495–502 (2015).
56. Doetsch F, Caille I, Lim DA, Garcia-Verdugo JM & Alvarez-Buylla A Subventricular zone astrocytes are neural stem cells in the adult mammalian brain. Cell 97, 703–16 (1999). [PubMed: 10380923]
57. Capilla-Gonzalez V, Cebrian-Silla A, Guerrero-Cazares H, Garcia-Verdugo JM & Quiñones-Hinojosa A Age-related changes in astrocytic and ependymal cells of the subventricular zone. Glia 62, 790–803 (2014). [PubMed: 24677590]
58. Jin Y-H & Kim BS Isolation of CNS-infiltrating and Resident Microglial Cells. Bio-protocol 5, e1385 (2015). [PubMed: 27148559]
59. Stubbington MJT et al. T cell fate and clonality inference from single-cell transcriptomes. Nature Methods 13, 329 (2016). [PubMed: 26950746]
60. Nakamura K et al. Sequence-specific error profile of Illumina sequencers. Nucleic Acids Research 39, e90–e90 (2011). [PubMed: 21576222]
61. Sergushichev AA An algorithm for fast preranked gene set enrichment analysis using cumulative statistic calculation. bioRxiv, 060012 (2016).

62. Finak G et al. MAST: a flexible statistical framework for assessing transcriptional changes and characterizing heterogeneity in single-cell RNA sequencing data. Genome Biology 16, 278 (2015). [PubMed: 26653891]

63. Robinson MD, McCarthy DJ & Smyth GK edgeR: a Bioconductor package for differential expression analysis of digital gene expression data. Bioinformatics 26, 139–140 (2010). [PubMed: 19910308]

64. Bittner S, Afzali AM, Wiendl H & Meuth SG Myelin oligodendrocyte glycoprotein (MOG35–55) induced experimental autoimmune encephalomyelitis (EAE) in C57BL/6 mice. Journal of visualized experiments : JoVE, 51275 (2014).

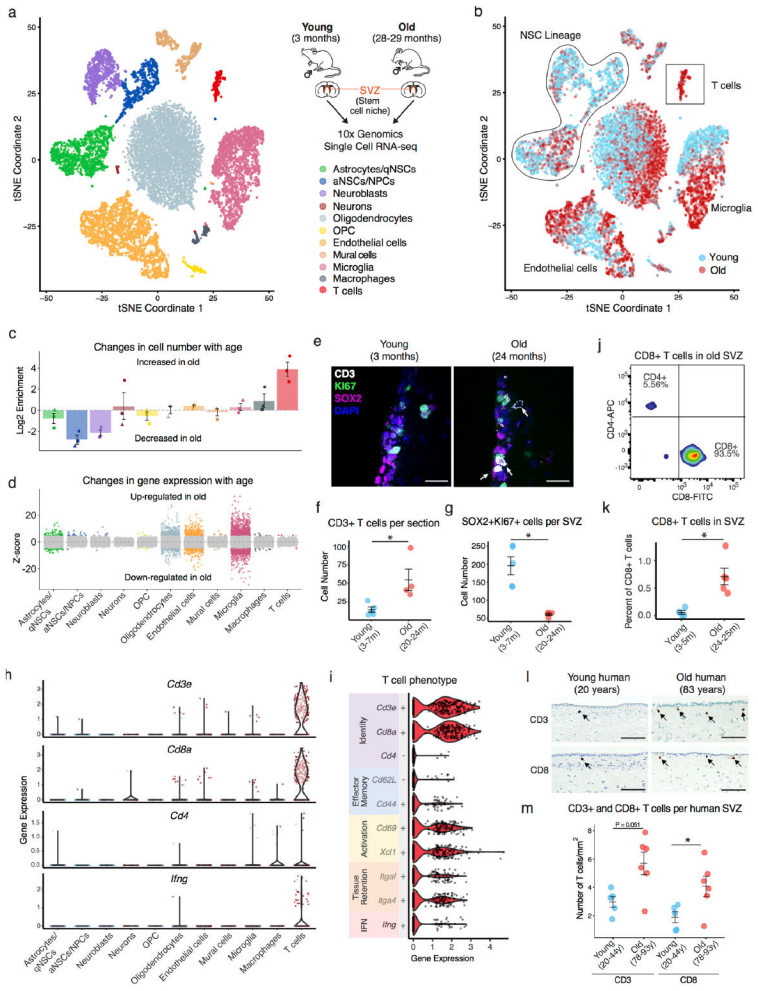

Figure 1 –. Single cell RNA-seq reveals changes in cell composition in old neurogenic niches, with infiltration of T cells in proximity to neural stem cells.

a) Single cell RNA-sequencing of the subventricular zone (SVZ) from 3 independent replicates of young (3 months) and old (28-29 months) perfused male mice using 10x Genomics Chromium. t-SNE clustering of 14,685 single cell transcriptomes (8,884 from young and 5,801 from old) colored by significant cell type clusters; **b)** t-SNE clustering as in a, but colored by age (for independent replicates, see Extended Data Fig. 1c); **c)** Age-dependent changes (log2 fold) in the percentage of each cell type. Data are mean +/− s.e.m. Each dot represents one replicate; **d)** Age-dependent changes in gene expression for each cell type. Each dot represents the differential expression MAST z-score of a gene. Dots with Bonferroni-corrected $P<0.05$ are in color; **e)** Immunofluorescence staining of the perfused SVZ neurogenic niche from young (3 months) and old (24 months) male mice. White: CD3 (T cells); Magenta: SOX2 (NSCs); Green: KI67 (cycling cells); Blue: DAPI (nuclei). Scale bar: 20 μm; **f, g)** Number of CD3+ T cells (f) and NSCs/NPCs (SOX2+KI67+) (g) per coronal section in 5 young (3-7 months) and 4 old (20-24 months) male mice. Data are mean +/− s.e.m. Each dot represents cells from one mouse. *P=0.020 (f), *P=0.016 (g), two-sided Wilcoxon rank sum test; **h)** Violin plot showing expression of *cd3 (cd3e)*, *cd8 (cd8a)*, *cd4*, and *ifng* in various cell types. Each dot represents expression levels in one cell. n=6 mice; **i)**

T cells exhibit markers of effector memory T cells (*Cd62L*^{low}, *Cd44*^{high}), activation (*Cd69+*, *Xcl1+*), tissue retention (*Itga1+, Itga4+*), and express interferon (*Ifng*). Each dot represents expression levels in one cell. n=6 mice; **j)** FACS plot of T cells in the SVZ of an old (24 months) male mouse. CD8+ T cells are defined as CD45+CD3+CD8+CD4−CD11b −B220−TER119−TCRγ/δ−; **k)** FACS quantification of the percentage of CD8+ T cells per SVZ in 4 young (3-5 months) and 5 old (24-25 months) male mice (combined over 2 independent experiments, Supplementary Table 12). Data are mean +/− s.e.m. Each dot represents T cells from one mouse. **P*=0.016, two-sided Wilcoxon rank sum test. **l)** Immunohistochemical staining for CD3 and CD8 (brown) in young (20 years) and old (83 years) human brain sections including the lateral ventricle, counterstained with hematoxylin (blue). Scale bar: 100 μm. **m)** Number of CD3+ (left) or CD8+ (right) T cells per unit area (mm^2) in proximity to the ventricle in 5 young (20-44 years) and 6 old (78-93 years) human brain sections of both sexes. Data are mean +/− s.e.m. Each dot represents T cells from one human specimen (Supplementary Table 4). **P*=0.030, two-sided Wilcoxon rank sum test.

Figure 2 –. T cells invading old brains are clonally expanded and differ from T cells in old blood.

a) CD8+ T cells from 6 old (24-29 months) male mice were FACS-isolated from the blood and perfused subventricular zones (SVZs) and analyzed by single cell RNA-sequencing using Smart-seq v4 (4 mice) or nested PCR (2 mice). Left: t-SNE plot of 247 CD8+ T cell transcriptomes, colored by source (blood=red and SVZ=orange). Each dot represents a single T cell transcriptome (n=4 old mice, 25-29 months); **b)** Expression of *Ifng* (IFNγ) and the checkpoint gene *Pdcd1* (PD-1), represented as log-normalized counts. Each dot represents expression levels in one single cell. n=247 cells from 4 old (25-29 months) mice. *Ifng* *** *FDR*=2.89×10^{-12}, *Pdcd1* *** *FDR*=1.29×10^{-40}, MAST differential expression test; **c, d)** Clonality of T cells in the blood or SVZs of old mice determined by TCR sequencing from Smart-seq v4 data using TraCeR (Mouse 1-4) (d) or by nested PCR of the TCR transcripts (Mouse 5, 6) (e). TCR-β sequence clones are ordered by decreasing frequency. T cell source is indicated in the bottom row. Dashed lines indicate transitions from expanded to unique TCR-β sequence clones; **e)** Percentage of T cells isolated from the SVZ or blood found in clones of increasing sizes; **f)** Venn diagram showing lack of overlap between T cell clones from old blood and brain (SVZ) for Mouse 1-4. Clones were designated as clonally expanded if the same TCR β-chain sequence was detected in multiple T cells.

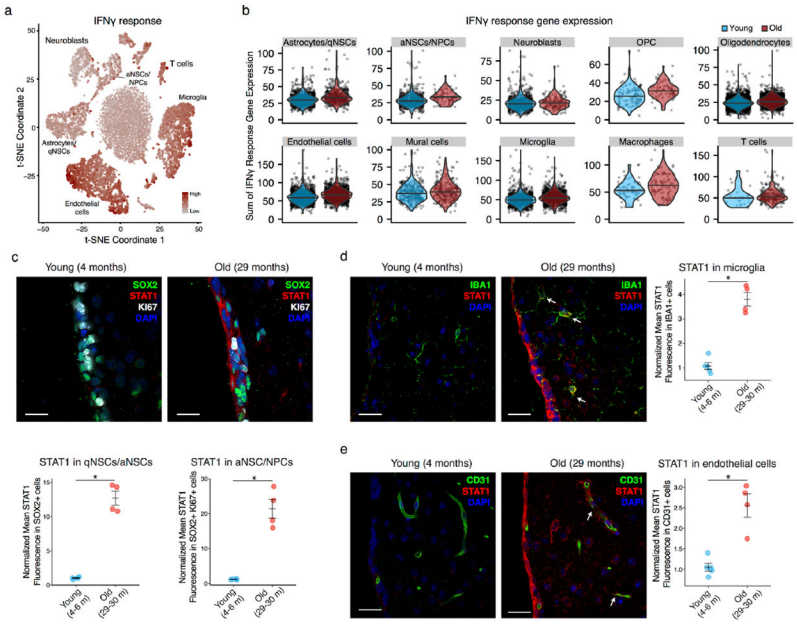

Figure 3 –. The neurogenic niche responds to IFN signaling.

a) t-SNE plot showing combined log-normalized expression values of genes in the IFNγ Response Hallmark from MSigDB (e.g. *Ifit1*, *Stat1*, and *Bst2*; Supplementary Table 8) in cells of the SVZ. Darker color indicates higher expression. n=14,685 cells clustered as in Fig. 1a; **b)** Combined log-normalized expression values of genes in IFNγ Response Hallmark in various cell types of the SVZ. Single cells were grouped by cell type and age (Supplementary Table 3). Median cellular IFNγ response values denoted by horizontal lines. Astrocytes/qNSCs $P<2.2\times10^{-16}$; aNSCs/NPCs $P=1.4\times10^{-9}$; Neuroblasts $P=0.056$, Endothelial $P<2.2\times10^{-16}$; Microglia $P<2.2\times10^{-16}$; T cells $P=0.230$, two-sided Wilcoxon rank sum test. **c-e)** Immunofluorescence staining of the IFN response gene STAT1 in different cell types in the SVZ of young (4 months) and old (29 months) male mice. Red: STAT1; Green: (c) SOX2 (NSCs), (d) IBA1 (microglia), or (e) CD31 (endothelial cells); White: KI67 (cycling cells); Blue: DAPI (nuclei). Scale bar: 20μm. Arrows: STAT1 staining in microglia and endothelial cells. **f-i)** Normalized STAT1 fluorescence intensity overlapping with cell marker fluorescence in 5 young (4-6 months) and 4 old (29-30 months) male mice. Data are mean +/− s.e.m. Each dot represents cells from one mouse. *$P=0.016$, two-sided Wilcoxon rank sum test.

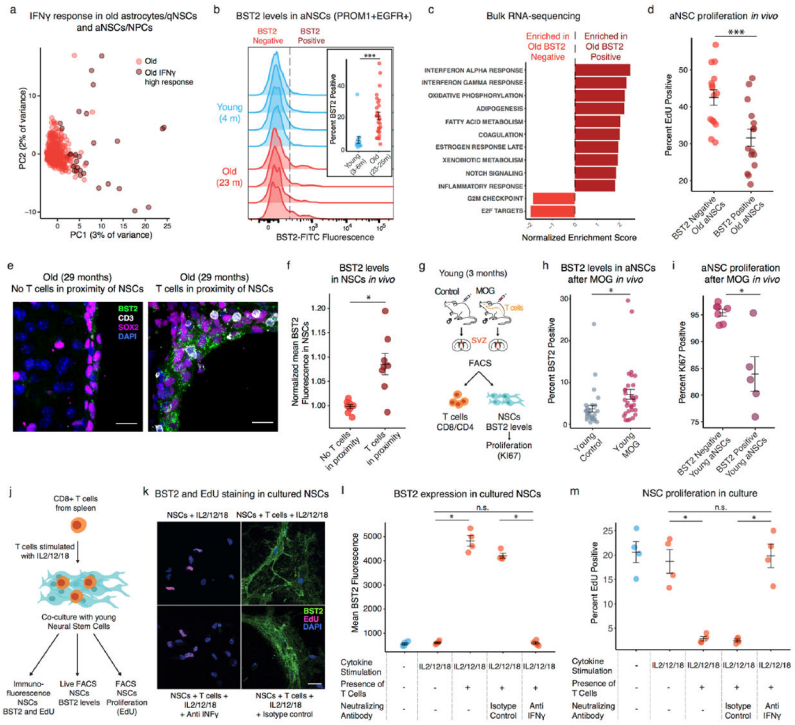

Figure 4. IFNγ signaling from T cells negatively impacts NSCs.

a) FACS histograms of BST2 fluorescence in aNSCs/NPCs from young (3 months, n=4) and old (24 months, n=4) mice. Inset: Percentage of aNSCs/NPCs that are BST2-positive of the ~500 cells analyzed from each young (n=15, 3-6 months) or old (n=28, 23-25 months) mouse (combined over 5 experiments, Supplementary Table 12). Data are mean +/− s.e.m. *** P=1.10 × 10^{-5}, two-sided Wilcoxon rank sum test; **b)** Hallmark gene set enrichment analysis of bulk RNA-seq from freshly isolated BST2-positive versus BST2-negative aNSCs/NPCs from old mice (24 months, n=4). For all pathways shown *FDR*<0.01, GSEA statistics; **c)** FACS quantification of the percentage of cells that are EdU positive (4 hours after EdU injection) of the ~100 BST2-positive and BST2-negative aNSCs/NPCs isolated from old male mice (n=15, 23-25 months) (combined over 3 experiments, Supplementary Table 12). Data are mean +/− s.e.m. Each dot represents cells from one mouse. *** P=3.23 × 10^{-4}, two-sided Wilcoxon rank sum test; **d)** Immunofluorescence staining of SVZ sections from an old (29 months) male mouse. White: CD3 (T cells); Magenta: SOX2 (NSCs): Green: BST2/Tetherin; Blue: DAPI (nuclei). Scale bar: 20 μm; **e)** Quantification of BST2 fluorescence in NSCs in proximity (or not) to CD3+ T cells in SVZ sections from 3 old (29-30 months) mice. Data represent mean +/− s.e.m. Each dot represents normalized BST2 fluorescence in SOX2+ NSCs in one section. ** P=0.007, two-sided Wilcoxon rank sum test. **f)** Scheme for co-culture of T cells and NSCs; **g)** Immunofluorescence staining of cultured NSCs from young mice (3 months) co-cultured with T cells and cytokines with or without the addition of a neutralizing antibody to IFNγ. Green: BST2 (high IFN response); Red: EdU (proliferating cells); Blue DAPI (nuclei). Scale bar: 20 μm; **h, i)** FACS quantification of the percentage of NSCs that are BST2-positive (h) or EdU-positive after a 4-hour pulse (i) of the ~1,000 cells analyzed from each NSC culture co-cultured with spleenic CD8+ T cells with or without addition of a neutralizing antibody to IFNγ. n=4 for each condition.

Representative of 2 independent experiments (see Supplementary Table 12). Data are mean +/− s.e.m. Each dot represents the mean fluorescence of an NSC culture derived from one mouse. *P=0.029, two-sided Wilcoxon rank sum test. n.s.=not significant.